HIV-1 Vpu restricts Fc-mediated effector functions in vivo

Jérémie Prévost[1,2], Sai Priya Anand[1,3], Jyothi Krishnaswamy Rajashekar[4], Jonathan Richard[1,2], Guillaume Goyette[1], Halima Medjahed[1], Gabrielle Gendron-Lepage[1], Hung-Ching Chen[5], Yaozong Chen[6], Joshua A. Horwitz[7,17], Michael W. Grunst[4], Susan Zolla-Pazner[8], Barton F. Haynes[9,10], Dennis R. Burton[11,12,13], Richard A. Flavell[14], Frank Kirchhoff[15], Beatrice H. Hahn[16], Amos B. Smith III[5], Marzena Pazgier[6], Michel C. Nussenzweig[7], Priti Kumar[4], Andrés Finzi[1,2,3,18,*]

[1]Centre de Recherche du CHUM, Montreal, QC H2X 0A9, Canada.
[2]Département de Microbiologie, Infectiologie et Immunologie, Université de Montréal, Montreal, QC H2X 0A9, Canada.
[3]Department of Microbiology and Immunology, McGill University, Montreal, QC H3A 2B4, Canada.
[4]Department of Internal Medicine, Section of Infectious Diseases, Yale University School of Medicine, New Haven, CT 06510, USA.
[5]Department of Chemistry, University of Pennsylvania, Philadelphia, PA 19104-6323, USA.
[6]Infectious Diseases Division, Department of Medicine, Uniformed Services University of the Health Sciences, Bethesda, MD 20814-4712, USA.
[7]Laboratory of Molecular Immunology, The Rockefeller University, New York, NY 10065, USA.
[8]Department of Medicine, Division of Infectious Diseases, Icahn School of Medicine at Mount Sinai, New York, NY 10029, USA.
[9]Duke Human Vaccine Institute, Departments of Medicine and Immunology, Duke University School of Medicine, Durham, NC 27710, USA.
[10]Consortium for HIV/AIDS Vaccine Development (CHAVD), Duke University, Durham, NC 27710, USA.
[11]Department of Immunology and Microbiology, The Scripps Research Institute, La Jolla, CA 92037, USA.
[12]Consortium for HIV/AIDS Vaccine Development (CHAVD), The Scripps Research Institute, La Jolla, CA 92037, USA.
[13]Ragon Institute of Massachusetts General Hospital, Massachusetts Institute of Technology, Harvard University, Cambridge, MA 02139, USA.
[14]Department of Immunobiology, Yale University School of Medicine, New Haven, CT, USA.
[15]Institute of Molecular Virology, Ulm University Medical Center, Ulm, 89081, Germany.
[16]Departments of Medicine and Microbiology, Perelman School of Medicine, University of Pennsylvania, Philadelphia, PA 19104-6076, USA.

[17]Current affiliation: Molecular Biology & Virology Group, PureTech Health LLC, Boston, MA 02210, USA.
[18]Lead contact

[*]**Correspondence:** andres.finzi@umontreal.ca (A.F.)

Key Words: HIV-1, Env, Vpu, non-neutralizing antibodies, broadly neutralizing antibodies, ADCC, CD4 mimetics, humanized mice

Word Count for Summary (maximum 150 words): 149

Total Character Count (maximum 45,000 characters): 45532

SUMMARY

Non-neutralizing antibodies (nnAbs) can eliminate HIV-1-infected cells via antibody-dependent cellular cytotoxicity (ADCC) and were identified as a correlate of protection in the RV144 vaccine trial. Fc-mediated effector functions of nnAbs were recently shown to alter the course of HIV-1 infection *in vivo* using a *vpu*-defective virus. Since Vpu is known to downregulate cell surface CD4, which triggers conformational changes in the viral envelope glycoprotein (Env), we ask whether the lack of Vpu expression was linked to the observed nnAbs activity. We found that restoring Vpu expression greatly reduces nnAb recognition of infected cells, rendering them resistant to ADCC responses. Moreover, administration of a nnAb in humanized mice reduces viral loads only in animals infected with a *vpu*-defective but not with a wildtype virus. Finally, nnAb Fc-effector functions are observed only on cells expressing Env in the "open" conformation. This work highlights the importance of Vpu-mediated evasion of humoral responses.

INTRODUCTION

Human immunodeficiency virus type 1 (HIV-1) envelope glycoproteins (Env) mediate viral entry into target cells. Env is synthesized as a trimeric gp160 precursor, which is further cleaved into two subunits linked by non-covalent bonds: the exterior gp120 and the transmembrane gp41 subunits (Earl et al., 1990; Freed et al., 1989; McCune et al., 1988). During the entry process, the gp120 subunit sequentially interacts with the CD4 surface molecule as well as one of its co-receptors (CCR5 or CXCR4) (Kwong et al., 1998; Shaik et al., 2019; Wu et al., 2010a), allowing the gp41 subunit to mediate fusion between the viral and target cell lipid membranes (Chan et al., 1997; Weissenhorn et al., 1997). Since Env is the sole viral antigen exposed at the surface of virions and infected cells, it represents the main target for humoral responses. Fusion-competent Env trimers can sample different conformations. Broadly neutralizing antibodies (bNAbs) mainly recognize the pre-fusion "closed" conformation (Li et al., 2020; Lu et al., 2019; Munro et al., 2014; Stadtmueller et al., 2018), while non-neutralizing antibodies (nnAbs) mainly bind to "open" CD4-bound conformations (Alsahafi et al., 2019; Jette et al., 2021; Munro et al., 2014; Yang et al., 2019). Primary difficult-to-neutralize HIV-1 isolates favor the pre-fusion “closed” conformation, thus exposing Env regions that are heavily glycan shielded (Doores, 2015; Lee et al., 2016; Li et al., 2020).

Since antiretroviral therapy (ART) is unable to eradicate HIV-1 reservoirs, monotherapy or combination of bNAbs targeting the CD4-binding site (3BNC117, VRC01, VRC07-523), the V3 glycan supersite (10-1074, PGT121) and the V2 apex (PGDM1400) are currently under investigation in multiple clinical trials as therapeutic agents to reduce or eliminate cellular reservoirs through Fc-mediated effector functions (NCT02140255, NCT03837756,

NCT04319367, NCT03721510). Thus far, results have shown that bNAbs can control HIV-1 viremia and delay viral rebound upon treatment interruption in HIV-1 infected individuals (Bar et al., 2016; Caskey et al., 2015; Caskey et al., 2017; Lynch et al., 2015; Scheid et al., 2016). Similar outcomes were also observed in non-human primates (NHP) and humanized mice (Barouch et al., 2013; Bolton et al., 2016; Freund et al., 2017; Halper-Stromberg et al., 2014; Hessell et al., 2016; Horwitz et al., 2013; Klein et al., 2012; Nishimura et al., 2017; Parsons et al., 2019; Schommers et al., 2020; Schoofs et al., 2019; Shingai et al., 2013). *In vivo* studies in animal models have demonstrated that Fc-mediated effector functions are required for the optimal therapeutic activity of bNAbs (Asokan et al., 2020; Bournazos et al., 2014; Halper-Stromberg et al., 2014; Lu et al., 2016; Wang et al., 2020). However, bNAbs rarely arise during natural infection and have yet to be consistently elicited by vaccination (Landais and Moore, 2018; Pauthner et al., 2019).

Given the difficulty of eliciting bNAbs *in vivo*, nnAbs have been evaluated as a potential alternative. nnAbs represent the majority of antibodies in the plasma of HIV-1-infected individuals and are easily elicited by vaccination (Beaudoin-Bussieres et al., 2020; Davis et al., 2009; Decker et al., 2005; Madani et al., 2016; Madani et al., 2018; Tomaras and Haynes, 2009; Tomaras et al., 2008; Visciano et al., 2019). Despite poor neutralization capacity, nnAbs can mediate other functions, such as the elimination of HIV-1-infected cells by antibody-dependent cellular cytotoxicity (ADCC) or antibody-dependent cellular phagocytosis (ADCP). Among these functions, ADCC was associated with the protection observed in the RV144 vaccine trial (Haynes et al., 2012a; Rerks-Ngarm et al., 2009). Thus, several studies have examined the antiviral effects of nnAbs in non-human primates and humanized mice. These included

prophylactic administration of nnAbs targeting the CD4-binding site (b6), the V3 loop (KD-247, 2219), the V1V2 region (830A, 2158), the gp120 cluster A (A32) and the gp41 immunodominant region (246D, 4B3, F240, 7B2). The results from these studies showed a reduction in the number of transmitted/founder (T/F) viruses and/or plasma viral loads after challenge with lab-adapted tier 1 viruses (Burton et al., 2011; Eda et al., 2006; Hessell et al., 2018; Hioe et al., 2022; Moog et al., 2014; Santra et al., 2015). Finally, therapeutic administration of large quantities of the monoclonal anti-gp41 246D nnAb to humanized mice infected with a *vpu*-deleted tier 2 HIV-1 molecular clone (HIV-$1_{NL4/3}$YU2) led to the elimination of infected cells and selected for escape mutations that stabilized Env "closed" conformation in an Fc-dependent manner, suggesting a protective effect (Horwitz et al., 2017). However, other studies administrating a cocktail of nnAbs (A32 and 17b) to humanized mice infected with a wild-type tier 2 HIV-1 strain (JR-CSF) had no impact on viral replication, except when combined with a small CD4 mimetic compound (CD4mc) that "open-up" the trimer and expose these otherwise occluded epitopes (Rajashekar et al., 2021).

Differences between the various nnAb studies could be attributed to the specificity of the antibodies (anti-gp41 vs anti-gp120), the humanized mouse model used or specific viral determinants. In particular, certain studies conducted using an infectious molecular clone (IMC) of HIV-1 that expressed a tier 2 Env (YU2) lacked a functional Vpu (HIV-$1_{NL4/3}$YU2). However, Vpu plays an important role in downregulating cell surface CD4, which can bind and trigger conformational changes in the viral Env, therefore exposing vulnerable epitopes (Prevost et al., 2022; Veillette et al., 2015; Veillette et al., 2014). We thus asked whether the lack of a functional Vpu was responsible for the observed nnAbs activity by comparing isogenic viruses that differed

130 solely in Vpu expression. Importantly, we tested the influence of Vpu expression on nnAb
131 function not only *in vitro* but also in humanized mice. We found that anti-gp41 246D nnAb
132 mediates potent ADCC responses against HIV-$1_{NL4/3}$YU2, but not its Vpu+ counterpart.
133 Accordingly, 246D was found to alter viral replication *in vivo* only in absence of Vpu. These
134 data thus provide conclusive evidence that Vpu allows HIV-1 to evade humoral responses and
135 emphasizes the need to use fully functional IMCs to assess nnAb Fc-mediated effector functions.
136

RESULTS

Elicitation of anti-gp41 non-neutralizing antibodies following immunization or HIV-1-infection.

First, we characterized the susceptibility of the HIV-$1_{NL4/3}$YU2 IMC to nnAbs-mediated Fc-effector responses to confirm previous observations (Horwitz et al., 2017). To do so, we used plasma samples from a cross-sectional cohort of 50 HIV-1-infected individuals (HIV+ plasma) which were grouped according to the inferred time post-infection and ART treatment (**Table S1**). The nnAbs present in the HIV+ plasma from this cohort were previously shown to mediate potent ADCC responses against infected cells presenting Env in the "open" CD4-bound conformation (Ding et al., 2016a; Richard et al., 2015; Veillette et al., 2015). We infected primary CD4+ T cells with the HIV-$1_{NL4/3}$YU2 IMC and evaluated the ability of HIV+ plasma to recognize and eliminate infected cells. Consistent with its susceptibility to nnAbs, HIV-$1_{NL4/3}$YU2-infected primary CD4+ T cells were efficiently recognized (**Figure 1A**) and susceptible to ADCC (**Figure 1B**) mediated by all the tested plasma samples, with a significant increase of activity starting six months post-infection. Similar levels of activity were also present in plasma from ART-treated individuals (**Figure 1A-B**).

Since the HIV-$1_{NL4/3}$YU2 IMC has been reported to be sensitive to anti-gp41 Fc-mediated antiviral activity *in vivo* (Horwitz et al., 2017), we evaluated the contribution of anti-gp41 nnAbs present in HIV+ plasma to infected-cell recognition and ADCC activity by performing binding competition experiments (**Figure 1C-D**). We focused on two main classes of anti-gp41 nnAbs based on observations from previous studies showing potent ADCC responses (Ding et al., 2016a; Gohain et al., 2016; Moog et al., 2014; Santra et al., 2015; Sojar et al., 2019; von Bredow

et al., 2016; Williams et al., 2019; Yang et al., 2018): anti-cluster I Abs targeting the disulfide loop region (C-C loop) (Gohain et al., 2016; Santra et al., 2015) and the anti-cluster II Abs targeting the heptad repeat region 2 (HR2) (Frey et al., 2010) (**Figure S1A**). Anti-gp41 cluster II nnAbs, inferred from binding competition experiments using the prototypic anti-cluster II 2.2B nnAb, were elicited in the acute phase of the infection (within 90 days) (**Figure 1D**). Elicitation of anti-gp41 cluster I nnAbs appears to take more time as revealed in binding competition experiments using the prototypic F240 anti-cluster I nnAb. While some competition with F240 binding was observed within the first three months post-infection, it culminates in the chronic phase of the infection (more than 2 years) (**Figure 1C**). In agreement with previous studies showing potent ADCC activity by anti-cluster I gp41 monoclonal Abs (Ding et al., 2016a; Gohain et al., 2016; Moog et al., 2014; Santra et al., 2015; von Bredow et al., 2016; Williams et al., 2019), we observed that blockade with anti-cluster I gp41 F240 Fab fragment significantly decreased plasma binding, FcγRIIIa engagement and ADCC responses against HIV-$1_{NL4/3}$YU2 infected cells (**Figure 1E-G**).

Vpu protects HIV-1-infected cells from recognition and Fc-effector functions mediated by anti-Env antibodies *in vitro* and *ex vivo*.

Since the HIV-$1_{NL4/3}$YU2 does not express the accessory protein Vpu due to a mutation in the start codon of the *vpu* gene (Horwitz et al., 2017), we asked whether the efficient recognition and ADCC-mediated elimination of HIV-$1_{NL4/3}$YU2 infected primary CD4+ T cells by nnAbs was linked to the lack of Vpu expression by this IMC. We restored the *vpu* open reading frame (ORF, **Figure 2A**) and infected primary CD4+ T cells using both Vpu-negative (Vpu-) and Vpu-positive (Vpu+) constructs. Using a recently developed FACS-based intracellular staining

183 method (Prevost et al., 2022), we confirmed Vpu expression upon restoration of the *vpu* ORF
184 (**Figure 2B**). We also confirmed by intracellular staining the equivalent expression of Nef in
185 both IMCs (**Figure 2B**). Vpu efficiently downregulated cell-surface CD4 and BST-2 (**Figure**
186 **2C**). We also measured cell surface expression of NTB-A and PVR, which were shown to
187 modulate ADCC responses against HIV-1-infected cells (Prevost et al., 2019) and are
188 downregulated by Vpu (Matusali et al., 2012; Shah et al., 2010). As expected, Vpu expression
189 significantly downregulated their expression from the surface of primary CD4+ T cells from five
190 different healthy individuals (**Figure 2D-E**).
191
192 We next evaluated the effect of Vpu on the recognition and elimination of infected cells by
193 nnAbs. Consistent with the observed downmodulation of CD4 and BST-2, Vpu expression
194 strongly reduced the recognition of infected cells by monoclonal antibodies (mAb) targeting the
195 anti-gp41 cluster I (246D), the gp41 cluster II (M785U3) and the gp120 cluster A (A32) (**Figure**
196 **3A**). We extended these results to a panel of 27 nnAbs which yielded the same results (**Figure**
197 **3B-C**). As a measure of this panel of nnAbs to mediate Fc-effector functions, we examined their
198 ability to interact with a soluble dimeric FcγRIIIa protein. This recombinant protein is used as a
199 surrogate of FcγR clustering which is required to trigger Fc-effector functions (Anand et al.,
200 2019; Wines et al., 2017; Wines et al., 2016). Consistent with a significant reduction in the
201 recognition of infected cells by nnAbs, we observed that Vpu expression diminished the ability
202 of all mAbs to engage with FcγRIIIa (**Figure 3D-E**) and to mediate ADCC (**Figure 3F-G**). We
203 noted that nnAbs targeting the gp41 were more potent at engaging soluble dimeric FcγRIIIa and
204 mediating ADCC against cells infected with the *vpu*-defective IMC than the panel of anti-gp120
205 nnAbs tested (**Figure S2A-C**).

Vpu facilitates viral release by downregulating the restriction factor BST-2 (Neil et al., 2008; Van Damme et al., 2008). Multiple studies have shown that this activity decreases the overall amount of Env at the cell surface, consequently decreasing the susceptibility of infected cells to ADCC (Alvarez et al., 2014; Arias et al., 2014; Pham et al., 2016; Richard et al., 2017; Veillette et al., 2014). Since the *vpu*-defective HIV-$1_{NL4/3}$YU2 was used to evaluate the *in vivo* activity of several bNAbs (Bournazos et al., 2016; Bournazos et al., 2014; Diskin et al., 2013; Freund et al., 2015; Freund et al., 2017; Halper-Stromberg et al., 2014; Horwitz et al., 2013; Klein et al., 2012; Klein et al., 2014; Lu et al., 2016; Schommers et al., 2020; Schoofs et al., 2019; Vanshylla et al., 2021), we tested whether their binding to infected cells was also influenced by Vpu expression. Consistent with decreased Env expression on cells infected with a Vpu+ virus, we observed a significant reduction in CD4-binding site (3BNC117), V3 glycan (10-1074) and V2-apex (PG16) bNAb binding (**Figure 4A**). The phenotype was validated using a panel of 35 bNAbs targeting different epitopes, indicative of an overall reduction of cell-surface Env expression in the presence of a functional Vpu (**Figure 4B-C**). Accordingly, infected cells were significantly less susceptible to bNAbs-mediated Fc-effector functions (**Figure 4D-G**). Among the different classes of bNAbs, antibodies targeting the V3 glycan supersite, the CD4-binding site and the V2 apex demonstrated stronger ADCC-mediated killing of cells infected with the *vpu*-defective HIV-$1_{NL4/3}$YU2, compared with antibodies known to interact with the gp120 silent face, the gp120-gp41 interface or the gp41 membrane-proximal external region (MPER), despite similar levels of Env recognition (**Figure S2D-F**). These findings support previous observations indicating that in addition to Env recognition, the angle of approach of the antibody is important

to mediate ADCC as it modulates the exposure of the Fc region required to activate effector cells (Acharya et al., 2014; Tolbert et al., 2020).

Since all coding regions of the HIV-$1_{NL4/3}$YU2 IMC other than the *env* gene are derived from a lab-adapted proviral backbone, we wished to test unmodified HIV-1 primary isolates. Primary CD4+ T cells were infected with a panel of 13 infectious molecular clones coding for Vpu or not. This panel includes transmitted/founder (T/F) viruses, molecular clones derived during chronic infection, and IMCs from lab-adapted strains as controls (**Figure 5A-B**). Vpu expression consistently reduced nnAbs (246D and M785U3) and bNAbs (3BNC117 and 10-1074) recognition of infected cells, which in turn protected infected cells from ADCC responses mediated by all antibodies tested (**Figure 5A-B**). Env polymorphisms present in CH167 (E460), REJO (N334) and CH293 (T332, N334) viruses abrogated the capacity of bNAbs 3BNC117 or 10-1074 to recognize infected cells. Of note, while Vpu expression has a profound effect in the recognition of infected cells by all tested anti-Env antibodies, it did not affect their neutralization profile (**Figure S1B-C**).

To extend our observations to a more physiological model, we expanded patient-derived infected CD4+ T cells. Briefly, we isolated and activated primary CD4+ T cells from five ART-treated HIV-1-infected individuals. Viral replication upon reactivation was monitored by intracellular p24 staining and flow cytometry (**Figure 5C**). These endogenously-infected cells were protected from Fc-mediated effector functions mediated by nnAb 246D but remained susceptible to bNAb PGT121 (**Figure 5C**), in agreement with our *in vitro* results generated using a Vpu+ IMC (**Figure 5A-B**).

Vpu expression limits the antiviral activity of the 246D antibody in HIV-1-infected humanized mice.

To determine the impact of Vpu expression on 246D antiviral activities *in vivo*, we infected SRG-15 (SIRPA$^{h/m}$ Rag2$^{-/-}$ Il2rg$^{-/-}$ IL15$^{h/m}$) humanized mice (hu-mice) with HIV-1$_{NL4/3}$YU2 or its Vpu-competent counterpart. Similar to a previously used humanized mouse model (Horwitz et al., 2017), this hu-mice model supports HIV-1 replication and Fc-effector functions *in vivo* (Herndler-Brandstetter et al., 2017; Rajashekar et al., 2021). Immunodeficient mice engrafted with human peripheral blood lymphocytes (hu-PBL) were infected intraperitoneally (I.P.) with 30,000 plaque-forming units (PFU) of either virus (**Figure 6A**). Half of each cohort received subcutaneous (S.C.) injections of the 246D nnAb at days 2, 4 and 6 post-infection. Infected humanized mice were then monitored for plasma viral loads (PVLs). Both viruses replicated efficiently in SRG-15 hu-PBL mice, reaching on average 1x10^7 viral RNA copies/mL of plasma at 3 days post-infection (P.I.) (**Figure 6B**). While PVLs in mice infected with HIV-1$_{NL4/3}$YU2 stabilized after day 3, infection with the Vpu+ variant further increased PVLs to 3.5x10^7 copies/mL by day 10. A single administration of the 246D nnAb at day 2 resulted in a significant reduction in PVLs (~36-fold decrease) in hu-mice infected with the *vpu*-defective virus but not significantly in those infected with the *vpu*-competent virus (**Figure 6B**). 246D maximal inhibitory effect (~85-fold reduction) was reached 10 days post-infection with the *vpu*-defective virus. At the end of the experiment (day 11), 246D treatment induced on average a 41-fold decrease in PVLs in mice infected with the *vpu*-defective virus but no difference in hu-mice infected with the Vpu+ virus. These results highlight the role played by Vpu in promoting viral replication in presence of nnAbs.

Harnessing non-neutralizing antibody Fc-effector functions by improving epitope exposure and FcγRIIIa interaction.

Enhancing the affinity of the Fc fragment of antibodies for FcγRs was shown to increase Fc-effector functions of bNAbs in HIV-1-infected humanized mice (Bournazos et al., 2014; Wang et al., 2020). To evaluate if this strategy could apply to nnAbs, we introduced well-characterized IgG1 Fc mutations in the 246D heavy chain to modulate its interaction with FcγRs. The GRLR mutations (G236R/L328R) and the GASDALIE mutations (G236A/S239D/A330L/I332E) are respectively known to decrease and increase the affinity for activating FcγRs (Bournazos et al., 2014; Horton et al., 2010; Smith et al., 2012). To characterize these Fc variants, primary CD4+ T cells were infected with the HIV-$1_{NL4/3}$YU2 constructs expressing Vpu or not. As expected, Fc modifications did not alter the ability of 246D to recognize infected cells, but it modulated the interaction with the soluble dimeric FcγR probe, with the GRLR mutations abrogating FcγRIIIa binding and the GASDALIE mutations improving it (**Figure 7A-B**). Introduction of the GASDALIE mutations enhanced ADCC against cells infected with the *vpu*-defective virus. Interestingly, it also allowed 246D to mediate ADCC against cells infected with the Vpu+ IMC, while the unaltered native 246D failed to do so (**Figure 7C**). To evaluate if the 246D GASDALIE was able to mediate ADCC against cells infected with a primary isolate, we infected primary CD4+ T cells with the transmitted/founder virus CH058, a strain shown to be resistant to 246D-mediated ADCC responses (**Figure 5B**). CH058-infected cells were poorly recognized by 246D and resistant to ADCC mediated by all 246D Fc variants tested, including 246D GASDALIE (**Figure 7D-F**). Consistent with the role of Nef and Vpu in preventing the exposure of epitopes recognized by nnAbs, disruption of the expression of both accessory proteins

297 enhanced recognition and ADCC susceptibility of infected cells by 246D (**Figure 7D-F**). These
298 results agree with the requirement of Env-CD4 interaction to expose the gp41 cluster I region.
299 246D recognizes with picomolar affinity a highly conserved linear peptide
300 (^{596}WGCSGKLICTT^{606}) which corresponds to the gp41 C-C loop, located between HR1 and
301 HR2 helices (**Figure S3A-C**). This epitope is occluded in the "closed" Env trimer structure but
302 can be exposed upon CD4-triggered conformational changes (**Figure S3D-E**).
303
304 While it is becoming increasingly clear that HIV-1 successfully evades nnAbs responses by
305 keeping its Env in a "closed" conformation (Bruel et al., 2017; Dufloo et al., 2020; Veillette et
306 al., 2015; Veillette et al., 2014; von Bredow et al., 2016), new strategies are currently being
307 tested to harness their potential antiviral activity. Small CD4 mimetic compounds have been
308 optimized to "open up" Env trimers, therefore exposing otherwise occluded epitopes recognized
309 by nnAbs (Ding et al., 2019b; Fritschi et al., 2021; Jette et al., 2021; Laumaea et al., 2020;
310 Melillo et al., 2016). Using this strategy, CD4mc were shown to synergize with monoclonal
311 CD4i Abs or nnAbs found in plasma from infected individuals to eliminate HIV-1-infected cells
312 *in vitro*, *ex vivo* and *in vivo* in humanized mice (Alsahafi et al., 2019; Anand et al., 2019; Ding et
313 al., 2016b; Lee et al., 2015; Madani et al., 2018; Prevost et al., 2020b; Rajashekar et al., 2021;
314 Richard et al., 2016; Richard et al., 2017; Richard et al., 2015). Since 246D was unable to
315 efficiently recognize cells infected with a primary isolate, we combined it with the CD4mc
316 BNM-III-170, which greatly improved its capacity to bind to CH058-infected cells (**Figure 7G**).
317 Accordingly, FcγRIIIa engagement and ADCC responses against WT-infected cells were
318 significantly enhanced upon CD4mc addition (**Figure 7H-I**). Altogether, our results suggest that
319 Fc-effector functions mediated by nnAbs are limited by the occluded nature of their epitopes.
320

DISCUSSION

The HIV-1 accessory protein Vpu is a multi-functional protein that promotes viral replication by interfering with the intracellular trafficking of various host proteins (Dube et al., 2010). CD4 and BST-2 downregulation by Vpu was shown to increase viral release in cell culture systems (Bour et al., 1999; Neil et al., 2008; Van Damme et al., 2008). Humanized mouse models of acute HIV-1 infection using HIV-1-infected humanized mice confirmed the role of Vpu in promoting viral replication in the initial phase of infection (Dave et al., 2013; Sato et al., 2012; Yamada et al., 2018). Similarly, chronic infection of NHPs with SHIV constructs encoding a defective or mutated *vpu* gene were found to be less pathogenic and exhibit lower viral loads (Hout et al., 2005; Shingai et al., 2011). In these *in vivo* studies, elevated viral loads were linked to Vpu-mediated CD4 and BST-2 downregulation, but the potential contribution of nnAbs to PVLs were not addressed. Beyond its effect on viral release, Vpu protects HIV-1-infected cells from nnAbs-mediated ADCC responses by limiting the presence of Env-CD4 complexes at the plasma membrane (Prevost et al., 2022; Veillette et al., 2015; Veillette et al., 2014). Here, we show that Vpu enhances viral replication *in vivo* by limiting nnAbs recognition of infected cells and therefore their capacity to mediate Fc-effector functions. Beyond infected cell elimination, the absence of Vpu could also affect the level of circulating infectious viral particles. While we did not observe any changes in the neutralization by anti-gp41 nnAbs against virions produced in 293T cells *in vitro* (**Figure S1B-C**), one could speculate that the capacity of nnAbs to neutralize viral particles originating from primary cells could also be altered in the absence of Vpu. Indeed, CD4 incorporation into virions has been shown to sensitize them to neutralization by various CD4i mAbs and HIV-IG (Ding et al., 2019a). While this was observed with *nef*-defective viruses, CD4 incorporation is also modulated by Vpu expression and this could apply to *vpu*-

344 defective viruses (Levesque et al., 2003). Our results highlight the importance of carefully
345 selecting viruses for *in vitro* and *in vivo* studies, since several widely used HIV-1 strains are
346 defective for Vpu expression (e.g. HXB2, YU2, ADA) (Li et al., 1991; Shaw et al., 1984;
347 Theodore et al., 1996).
348
349 Different approaches aimed at generating bNAbs by vaccination are being investigated using
350 germline-targeting Env immunogens (Dosenovic et al., 2015; Jardine et al., 2016; Steichen et al.,
351 2016) followed by sequential Env trimer immunization (Escolano et al., 2016; Haynes et al.,
352 2012b; Saunders et al., 2019; Williams et al., 2017) to guide antibody maturation. However,
353 none of these vaccine studies have yet resulted in the consistent elicitation of bNAbs. Facing the
354 difficulty in eliciting bNAbs by vaccination, nnAbs have been studied as an alternative for
355 vaccine development. If ADCC activity contributes to vaccine protection, as suggested in the
356 RV144 trial (Haynes et al., 2012a), our results suggest that elicitation of nnAbs are unlikely to
357 confer protection in a vaccine setting unless strategies to "open" the Env trimer are in place.
358 Supporting this, NHP immunized with monomeric gp120 were completely protected from a
359 heterologous SHIV infection if a CD4mc was combined with the challenge viral stock (Madani
360 et al., 2018). This study showed that nnAbs elicited by the gp120 immunogen did not protect in
361 the absence of CD4mc.
362
363 In this study, we selected the SRG-15 humanized mouse model over other humanized mouse
364 models because of its endogenous expression of human IL-15, which allows the development of
365 a functional NK cell compartment (Herndler-Brandstetter et al., 2017). NK cells play a central
366 role in the ADCC responses *in vitro* and *in vivo*¸ and their specific depletion has been shown to

abrogate the elimination of HIV-1 reservoirs by a combination of CD4mc and nnAbs in SRG-15 humanized mice (Rajashekar et al., 2021). Human IL-15 expression likely also increases HIV-1 replication by regulating the susceptibility of CD4+ T cells to infection (Manganaro et al., 2018). This could explain the higher viral load peak (~10^7 copies/mL) (**Figure 6B**) compared to those achieved in the NRG humanized mice using the same HIV-$1_{NL4/3}$YU2 IMC (~10^5 copies/mL) in previous studies (Halper-Stromberg et al., 2014; Horwitz et al., 2017). We also used humanized mice as a model of HIV-1 infection since it allows the use of clinically-relevant HIV-1 isolates and does not require Env adaptation to replicate.

In addition to accessory proteins, Env conformation is a critical factor when studying nnAbs Fc-effector functions (Alsahafi et al., 2016; Ding et al., 2016a; Dufloo et al., 2020; Prevost et al., 2021; Prevost et al., 2018a; Prevost et al., 2018b; Prevost et al., 2017; Richard et al., 2015; Veillette et al., 2015; Veillette et al., 2014). Multiple studies reported significant effects of nnAbs in limiting HIV-1/SHIV replication *in vivo* using viruses coding for easy-to-neutralize tier 1 Env from lab-adapted strains, which are readily recognized by nnAbs (Burton et al., 2011; Eda et al., 2006; Hessell et al., 2018; Hioe et al., 2022; Moog et al., 2014; Santra et al., 2015). A recent study showed that tier 2 primary virus can be impacted *in vivo* by nnAbs but only when combined with CD4mc (Rajashekar et al., 2021). This combination of nnAbs and CD4mc significantly reduced plasma viral loads and the size of the viral reservoir in an Fc-effector functions and NK cells dependent manner (Rajashekar et al., 2021). These results emphasize the need to utilize fully functional viruses in ADCC assays to preclude Vpu-related artifacts. However, one could speculate that the development of broad-spectrum Vpu inhibitors may enhance the efficacy of nnAbs to eliminate HIV-1-infected cells (Robinson et al., 2021). Overall,

390 our study indicate that it is unlikely for nnAbs-based immunotherapies to alter viral replication in
391 the absence of strategies aimed at exposing the vulnerable epitopes they recognize.
392

ACKNOWLEDGMENTS

The authors thank the CRCHUM BSL3 and Flow Cytometry Platforms for technical assistance, and Mario Legault from the FRQS AIDS and Infectious Diseases network for cohort coordination and clinical samples. We thank the following collaborators for kindly providing antibodies: Julie Overbaugh (Fred Hutchinson Cancer Research Center) for QA255-006, QA255-067 and QA255-072, James Robinson (Tulane University) for 7B2, 2.2B, 12.3D, 12.4H, A32, C11 and 17b, George Lewis (University of Maryland) for M785U1, M785U2, M785U3, M785U4, N5U1, N5U2, N5U3, N10U1 and N10U2, Gunilla Karlsson Hedestam (Karolinska Institutet) for GE2-JG8, John Mascola (Vaccine Research Center, NIAID) for VRC01, VRC03, VRC07-523, VRC13, VRC16 and VRC34, Mark Connors (NIAID) for 10E8, N6 and 35O22, Florian Klein (University of Cologne) for 1-18, and the International AIDS Vaccine Initiative (IAVI) for PG9, PG16, PGT121, PGT122, PGT123, PGT125, PGT126, PGT128, PGT130, PGT135, PGT136, PGT145 and PGT151. We thank P. Mark Hogarth (Burnet Institute) for kindly providing recombinant dimeric FcγRIIIa. The Figure 6 was prepared using illustrations from BioRender.com.

This study was supported by a Canadian Institutes of Health Research (CIHR) foundation grant #352417 to A.F. Funds were also provided by a CIHR Team grant #422148 to P.K. and A.F., a Canada Foundation for Innovation (CFI) grant #41027 to A.F and by the National Institutes of Health to A.F. (R01 AI148379 and R01 AI150322), to M.P. and A.F. (R01 AI129769), M.P. (AI116274) and to P.K. (R01 AI145164, R33 AI122384 and P50 AI150464 [CHEETAH]). Support for this work was also provided by P01 GM56550/AI150471 to A.B.S. and A.F. This work was partially supported by 1UM1AI164562-01, co-funded by National Heart, Lung and

Blood Institute, National Institute of Diabetes and Digestive and Kidney Diseases, National Institute of Neurological Disorders and Stroke, National Institute on Drug Abuse and the National Institute of Allergy and Infectious Diseases to A.F. A.F. is the recipient of a Canada Research Chair on Retroviral Entry #RCHS0235 950-232424. F.K. is supported by the German Research Foundation (DFG CRC 1279 and SPP 1923) and the Baden-Württemberg Foundation (BWST-ISF2018-032). J.P. and S.P.A. are recipients of CIHR doctoral fellowships. M.W.G. is a recipient of the Gruber Science Fellowship. The funders had no role in study design, data collection and analysis, decision to publish, or preparation of the manuscript.

AUTHOR CONTRIBUTIONS

Conceptualization: J.P. and A.F.; **Methodology:** J.P., J.K.R., P.K. and A.F.; **Investigation:** J.P., S.P.A., J.K.R., J.R., G.G., H.M., G.G.-L., Y.C. and M.W.G.; **Resources:** J.P., H.-C.C., J.A.H., S.Z.-P., B.F.H., D.R.B., R.A.F., F.K., B.H.H., A.B.S., M.P., M.C.N., P.K. and A.F.; **Formal Analysis:** J.P.; **Visualization:** J.P.; **Supervision:** A.B.S., M.P., M.C.N., P.K. and A.F.; **Funding acquisition:** A.B.S., M.P., P.K. and A.F.; **Writing – original draft:** J.P., B.H.H. and A.F.; **Writing – review & editing:** All authors.

DECLARATION OF INTERESTS

The authors declare no competing interests.

DISCLAIMER

437 The opinions and assertions expressed herein are those of the author(s) and do not necessarily
438 reflect the official policy or position of the Uniformed Services University or the Department of
439 Defense.
440

441 **FIGURE LEGENDS**

442

443 **Figure 1. Cells infected with HIV-1$_{NL4/3}$YU2 are susceptible to nnAb-mediated ADCC**
444 **responses.** Primary CD4+ T cells were either mock-infected (grey symbols) or infected with the
445 HIV-1$_{NL4/3}$YU2 virus (black symbols). (**A**) Cell-surface staining and (**B**) ADCC responses
446 mediated by plasma from 50 different HIV-1-infected individuals categorized by the time post-
447 infection and the antiretroviral therapy (ART) treatment status. (**A**) The graph shows the mean
448 fluorescence intensities (MFI) on the whole cell population (mock) or infected p24+ cell
449 population (HIV-1$_{NL4/3}$YU2). (**C-D**) The binding of Alexa Fluor 647 (AF647)-precoupled (**C**)
450 anti-gp41 cluster I F240 mAb or (**D**) anti-gp41 cluster II 2.2B mAb was evaluated in presence of
451 unlabeled human plasma from healthy controls or HIV-1-infected individuals. A pool of purified
452 immunoglobulins from HIV-1-infected individuals (HIV-IG) was used as a positive control. (**E**)
453 Plasma binding, (**F**) FcγRIIIa binding and (**G**) ADCC responses mediated by plasma from 10
454 untreated HIV-1-infected individuals (2-5 years) were evaluated in presence of competing anti-
455 gp41 cluster I F240 Fab fragment. Error bars indicate means ± standard errors of the means
456 (SEM). Statistical significance was tested using (**A-D**) one-way ANOVA with a Holm-Sidak
457 post-test or (**E-G**) a paired t test (*, $P < 0.05$; **, $P < 0.01$; ***, $P < 0.001$; ****, $P < 0.0001$; ns,
458 nonsignificant).

459

460 **Figure 2. Reversion of Vpu open reading frame in the HIV-1$_{NL4/3}$YU2 construct.**
461 (**A**) Sequence alignment of the Vpu open reading frame (ORF) region of selected HIV-1
462 reference isolates (NL4/3, HXB2, YU2) with the HIV-1$_{NL4/3}$YU2 construct and its Vpu+
463 counterpart. Identical nucleotides are shaded in dark gray, conserved nucleotides in light gray

and non-identical nucleotides are highlighted in red. The *vpu* start codon is highlighted by a black box. (**B-E**) Primary CD4+ T cells either mock-infected or infected with the HIV-$1_{NL4/3}$YU2 virus or its Vpu+ counterpart were stained for intracellular detection of (**B**,**D**) viral proteins Vpu and Nef and cell-surface detection of (**C**,**E**) cellular proteins CD4, BST-2, NTB-A and PVR. (**B-C**) Histograms depicting representative stainings for (**B**) viral proteins and (**C**) their target substrates. (**D-E**) The graphs show the mean fluorescence intensities (MFI) obtained from five independent experiments using primary cells from five different healthy donors. (**D**) Viral protein levels were reported as a fold increase in the signal detected on infected p24+ cells compared to uninfected p24- cells. (**E**) Cellular protein levels were reported as a percentage of detection at the surface of infected p24+ cells compared to uninfected p24- cells. Error bars indicate means ± standard errors of the means (SEM). Statistical significance was tested using an unpaired t test or a Mann-Whitney U test based on statistical normality (**, $P < 0.01$; ****, $P < 0.0001$; ns, nonsignificant).

Figure 3. Vpu expression impairs Env recognition and Fc-effector functions mediated by anti-Env nnAbs.

Primary CD4+ T cells were either mock-infected or infected with the HIV-$1_{NL4/3}$YU2 virus or its Vpu+ counterpart. (**A-E**) Cell surface staining performed using anti-gp41 non-neutralizing antibodies targeting the gp41 cluster I, cluster II or other gp41 regions as well as anti-gp120 CD4-induced antibodies. Antibody binding was detected either by using (**A-C**) Alexa Fluor 647-conjugated anti-human secondary Abs or (**D-E**) by using biotinylated recombinant soluble dimeric FcγRIIIa followed by the addition of Alexa Fluor 647-conjugated streptavidin. (**A**) Histograms depicting representative stainings using anti-gp41 cluster I 246D, anti-gp41 cluster II

M785U3 and anti-gp120 cluster A A32 mAbs. (**B**,**D**) The graphs represent the mean fluorescence intensities (MFI) obtained from the infected p24+ cell population using cells from five different healthy donors. (**D**) The horizontal dotted line represents the signal obtained in absence of mAb. (**F-G**) Primary CD4+ T cells infected with HIV-$1_{NL4/3}$YU2 viruses were used as target cells. Autologous PBMCs were used as effector cells in a FACS-based ADCC assay. (**F**) The graph represents the percentages of ADCC obtained in the presence of the respective antibodies using cells from five different healthy donors. Error bars indicate means ± standard errors of the means (SEM). (**C**,**E,G**) Statistical significance was tested using a paired t test (****, $P < 0.0001$).

Figure 4. Vpu expression decreases Env recognition and Fc-effector functions mediated by anti-Env bNAbs.

Primary CD4+ T cells were either mock-infected or infected with the HIV-$1_{NL4/3}$YU2 virus or its Vpu+ counterpart. (**A-E**) Cell surface staining performed using broadly neutralizing antibodies targeting the gp120 V3 glycan supersite, CD4 binding site, V2 apex and silent face, the gp120-gp41 interface and the gp41 MPER. Antibody binding was detected either by using (**A-C**) Alexa Fluor 647-conjugated anti-human secondary Abs or (**D-E**) by using biotinylated recombinant soluble dimeric FcγRIIIa followed by the addition of Alexa Fluor 647-conjugated streptavidin. (**A**) Histograms depicting representative stainings using anti-CD4 binding site 3BNC117, anti-V3 glycan 10-1074 and anti-V2 apex PG16 mAbs. (**B**,**D**) The graphs represent the mean fluorescence intensities (MFI) obtained from the infected p24+ cell population using cells from five different healthy donors. (**D**) The horizontal dotted line represents the signal obtained in absence of mAb. (**F-G**) Primary CD4+ T cells infected with HIV-$1_{NL4/3}$YU2 viruses were used as

target cells. Autologous PBMCs were used as effector cells in a FACS-based ADCC assay. (**F**) The graph represents the percentages of ADCC obtained in the presence of the respective antibodies using cells from five different healthy donors. Error bars indicate means ± standard errors of the means (SEM). (**C**,**E,G**) Statistical significance was tested using a paired t test (****, $P < 0.0001$).

Figure 5. The ability of Vpu to limit anti-Env ADCC responses is conserved among different HIV-1 strains.

(**A-B**) Primary CD4+ T cells were infected with HIV-1 clade B and clade C transmitted/founder (CH058, CH077, REJO, CH198, ZM246F), chronic (AD8, JRCSF, YU2, STCO, CH167, CH293) and lab-adapted (NL4/3, HIV-$1_{NL4/3}$YU2) wild-type (WT) strains or their Vpu-counterpart. (**A**) Cell surface staining performed using anti-gp41 nnAbs 246D and M785U3, as well as bNAbs 3BNC117 and 10-1074. Antibody binding was detected either by using Alexa Fluor 647-conjugated anti-human secondary Abs. (**B**) Infected primary CD4+ T cells were used as target cells and autologous PBMCs were used as effector cells in a FACS-based ADCC assay. (**C**) Primary CD4+ T cells from five different ART-treated HIV-1-infected individuals were isolated and activated with PHA-L/IL-2 to expand the endogenous virus. Cell surface staining and ADCC experiments were performed upon reactivation. Antibody binding was detected using Alexa Fluor 647-conjugated anti-human secondary Abs or biotinylated recombinant soluble dimeric FcγRIIIa followed by the addition of Alexa Fluor 647-conjugated streptavidin. *Ex vivo*-expanded infected primary CD4+ T cells from four HIV-1-infected individuals were used as target cells and autologous PBMCs were used as effector cells in a FACS-based ADCC assay. ADCC susceptibility was only measured when the percentage of infection (p24+ cells) was

higher than 10%. (**A,C**) The horizontal dotted lines represent the signal obtained in absence of mAb. (**A-C**) The antibody binding and FcγRIIIa graphs represent the mean fluorescence intensities (MFI) obtained from the infected p24+ cell population. The ADCC graphs represent the percentages of ADCC obtained in the presence of the respective antibodies. Error bars indicate means ± standard errors of the means (SEM). Statistical significance was tested using (**A-B**) a paired t test or Wilcoxon signed-rank test based on statistical normality or (**C**) a Mann-Whitney U test (*, $P < 0.05$; **, $P < 0.01$; ***, $P < 0.001$; ****, $P < 0.0001$; ns, nonsignificant).

Figure 6. Vpu promotes HIV-1 replication in humanized mice treated with non-neutralizing antibody 246D.

(**A**) Experimental outline. SRG-15-Hu-PBL mice were infected with HIV-$1_{NL4/3}$YU2 or its Vpu+ counterpart intraperitoneally. At day 2, 4 and 6 post-infection, mice were administered 1mg of 246D mAb subcutaneously (S.C.). Mice were bled routinely for plasma viral load (PVL) quantification. (**B**) PVL levels were measured by quantitative real-time PCR (limit of detection = 300 copies/mL, dotted line). Twelve mice were infected using each virus; six of them were mock-treated (black lines) and the other six were treated with 246D mAb (gray lines). PVL measurements for individual mice are shown as dashed lines and mean values for each regimen are shown as solid lines. Statistical significance was tested using an unpaired t test or a Mann-Whitney U test based on statistical normality (*, $P < 0.05$;**, $P < 0.01$; ns, nonsignificant).

Figure 7. CD4 mimetics and Fc modifications boost the capacity of anti-gp41 nnAbs to mediate ADCC responses. Primary CD4+ T cells were either infected with (**A-C**) HIV-$1_{NL4/3}$YU2 virus or its Vpu+ counterpart, (**D-F**) transmitted/founder virus CH058 wild-type (WT)

or its Nef and/or Vpu-deleted counterparts (N-, U-, N-U-) or (**G-I**) CH058 WT with further treatment or not with CD4mc BNM-III-170 during staining and ADCC experiments. Cell surface staining performed using anti-gp41 nnAb 246D WT or Fc-mutated to impair (G236R/L328R; GRLR) or enhance (G236A/S239D/A330L/I332E; GASDALIE) Fc-effector functions. Antibody binding was detected using (**A**,**D**,**G**) Alexa Fluor 647-conjugated anti-human secondary Abs or (**B**,**E**,**H**) by using biotinylated recombinant soluble dimeric FcγRIIIa followed by the addition of Alexa Fluor 647-conjugated streptavidin. (**A-B**,**D-E**,**G-H**) The graphs represent the mean fluorescence intensities (MFI) obtained from the infected p24+ cell population using cells from five different healthy donors. (**B,E,H**) The horizontal dotted lines represent the signal obtained in absence of mAb. (**C**,**F**,**I**) Infected primary CD4+ T cells were used as target cells and autologous PBMCs were used as effector cells in a FACS-based ADCC assay. The graphs represent the percentages of ADCC obtained in the presence of the respective antibodies using cells from five different healthy donors. Error bars indicate means ± standard errors of the means (SEM). (**A-I**) Statistical significance was tested using a one-way ANOVA with a Holm-Sidak post-test or a Kruskal-Wallis test with a Dunn's post-test when comparing between the different 246D Fc variants and (**C**) an unpaired t test or a Mann-Whitney U test when comparing between viruses or treatment. Appropriate statistical test (parametric or nonparametric) was applied based on dataset distribution normality (*, $P < 0.05$; **, $P < 0.01$; ***, $P < 0.001$; ****, $P < 0.0001$; ns, nonsignificant).

STAR METHODS

KEY RESOURCES TABLE

REAGENT or RESOURCE	SOURCE	IDENTIFIER
Antibodies		
Monoclonal anti-Env gp41 246D	NIH AIDS Reagent Program (Xu et al., 1991)	N/A
Monoclonal anti-Env gp41 246D GRLR	This paper	N/A
Monoclonal anti-Env gp41 246D GASDALIE	This paper	N/A
Monoclonal anti-Env gp41 F240	NIH AIDS Reagent Program (Cavacini et al., 1998)	Cat# 7623
Anti-Env gp41 F240 Fab fragment	(Gohain et al., 2016)	N/A
Monoclonal anti-Env gp41 240D	NIH AIDS Reagent Program (Xu et al., 1991)	Cat# 1242
Monoclonal anti-Env gp41 167D	NIH AIDS Reagent Program (Xu et al., 1991)	Cat# 11681
Monoclonal anti-Env gp41 50-69	NIH AIDS Reagent Program (Gorny et al., 1989)	Cat# 531
Monoclonal anti-Env gp41 QA255-006, QA255-067 and QA255-072	Dr Julie Overbaugh (Williams et al., 2019)	N/A
Monoclonal anti-Env gp41 7B2	NIH AIDS Reagent Program	Cat# 12556
Monoclonal anti-Env gp41 2.2B, 12.3D and 12.4H	Dr James E. Robinson	N/A
Monoclonal anti-Env gp41 M785U1, M785U2, M785U3, M785U4, N10U1, N10U2, N5U1, N5U2 and N5U3	Dr George Lewis (Ding et al., 2016a)	N/A
Monoclonal anti-Env cluster A A32	NIH AIDS Reagent Program	Cat# 11438
Monoclonal anti-Env cluster A N5i5	(Guan et al., 2013)	N/A
Monoclonal anti-Env cluster A C11	Dr James E. Robinson (Robinson JE, 1992)	N/A
Monoclonal anti-Env co-receptor binding site 17b	NIH AIDS Reagent Program	Cat# 4091
Monoclonal anti-Env co-receptor binding site X5	(Huang et al., 2004)	N/A
Monoclonal anti-Env V3 loop GE2-JG8	Dr Gunilla Karlsson Hedestam (Phad et al., 2015)	N/A
Monoclonal anti-Env CD4 binding site 3BNC117	(Scheid et al., 2011)	RRID:AB_2491033

Monoclonal anti-Env CD4 binding site N49-P7	(Sajadi et al., 2018)	N/A
Monoclonal anti-Env CD4 binding site VRC01	NIH AIDS Reagent Program (Wu et al., 2010b)	Cat# 12033; RRID:AB_2491019
Monoclonal anti-Env CD4 binding site VRC03	NIH AIDS Reagent Program (Wu et al., 2010b)	Cat# 12032; RRID:AB_2491021
Monoclonal anti-Env CD4 binding site VRC07-523	Dr John Mascola (Rudicell et al., 2014)	N/A
Monoclonal anti-Env CD4 binding site VRC13 and VRC16	Dr John Mascola (Zhou et al., 2015)	N/A
Monoclonal anti-Env CD4 binding site N6	NIH AIDS Reagent Program (Huang et al., 2016)	Cat# 12968
Monoclonal anti-Env CD4 binding site NC-Cow1	(Sok et al., 2017)	RRID:AB_2687423
Monoclonal anti-Env CD4 binding site b12	NIH AIDS Reagent Program (Burton et al., 1994)	Cat# 2640; RRID:AB_2491069
Monoclonal anti-Env CD4 binding site 1-18	Dr Florian Klein (Schommers et al., 2020)	N/A
Monoclonal anti-Env CD4 binding site HJ16	NIH AIDS Reagent Program (Corti et al., 2010)	Cat# 12138; RRID:AB_2491032
Monoclonal anti-Env CD4 binding site CH106	NIH AIDS Reagent Program (Liao et al., 2013)	Cat# 12566
Monoclonal anti-Env V3 glycan PGT121, PGT122, PGT123, PGT125, PGT126, PGT128, PGT130, PGT135 and PGT136	International AIDS Vaccine Initiative (Walker et al., 2011)	RRID:AB_2491041 RRID:AB_2491042 RRID:AB_2491043 RRID:AB_2491044 RRID:AB_2491045 RRID:AB_2491047 RRID:AB_2491048 RRID:AB_2491050 RRID:AB_2491060
Monoclonal anti-Env V3 glycan BG18	(Freund et al., 2017)	N/A
Monoclonal anti-Env V3 glycan 10-1074	(Mouquet et al., 2012)	RRID:AB_2491062
Anti-Env V2 apex PGT145 monoclonal Ab	International AIDS Vaccine Initiative (Walker et al., 2011)	RRID:AB_2491054
Anti-Env V2 apex PG9 and PG16 monoclonal Ab	International AIDS Vaccine Initiative (Walker et al., 2009)	RRID:AB_2491030 RRID:AB_2491031
Anti-Env silent face SF12 monoclonal Ab	(Schoofs et al., 2019)	N/A
Monoclonal anti-Env gp120-gp41 interface PGT151	International AIDS Vaccine Initiative (Falkowska et al., 2014)	N/A

Monoclonal anti-Env gp120-gp41 interface 8ANC195	(Scheid et al., 2011)	RRID:AB_2491037
Monoclonal anti-Env gp120-gp41 interface 35O22	Dr Mark Connors (Huang et al., 2014)	N/A
Monoclonal anti-Env gp120-gp41 interface VRC34	Dr John Mascola (Kong et al., 2016)	RRID:AB_2819225
Monoclonal anti-Env gp41 MPER 10E8	NIH AIDS Reagent Program (Huang et al., 2012)	Cat# 12294; RRID:AB_2491067
Monoclonal anti-Env gp41 MPER 4E10	NIH AIDS Reagent Program (Stiegler et al., 2001)	Cat# 10091; RRID:AB_2491029
Monoclonal anti-Env gp41 MPER 2F5	NIH AIDS Reagent Program (Buchacher et al., 1994)	Cat# 1475; RRID:AB_2491015
Polyclonal Anti-HIV Immune Globulin, Pooled Inactivated Human Sera (HIV-IG)	NIH AIDS Reagent Program	Cat# 3957; RRID:AB_2890264
Mouse anti-Human CD4 clone OKT4	Thermo Fisher Scientific	Cat# 14-0048-82; RRID:AB_467075
PE-Cy7 Mouse anti-Human CD317 (BST-2) clone RS38E	Biolegend	Cat# 348416; RRID:AB_2716221
Mouse anti-human CD155 (PVR) clone SKII.4	Biolegend	Cat# 337602; RRID:AB_2300508
Mouse anti-human CD352 (NTB-A) clone NT-7	Biolegend	Cat# 317202; RRID:AB_571931
Rabbit Anti-HIV-1 Nef Polyclonal Antibody	NIH AIDS Reagent Program	Cat# 2949
Rabbit Anti-HIV-1 Vpu Polyclonal Antibody	(Prevost et al., 2020a)	N/A
Goat anti-Human IgG (H+L) Cross-Adsorbed Secondary Antibody, Alexa Fluor 647	Thermo Fisher Scientific	Cat# A21445; RRID:AB_2535862
Goat anti-Mouse IgG (H+L) Cross-Adsorbed Secondary Antibody, Alexa Fluor 647	Thermo Fisher Scientific	Cat# A21235; RRID:AB_2535804
Alexa Fluor 647 anti-Human IgG Fc Antibody	Biolegend	Cat# 409319; RRID:AB_2563329
Brilliant Violet 421 Donkey anti-Rabbit IgG (minimal x-reactivity) Antibody	Biolegend	Cat# Poly4064; RRID:AB_10643424
Goat anti-Human IgG Fc Cross-Adsorbed Secondary Antibody, HRP	Thermo Fisher Scientific	Cat# A18823; RRID:AB_2535600
Streptavidin, Alexa Fluor 647 conjugate	Thermo Fisher Scientific	Cat# S32357; RRID:AB_2336066
PE Mouse anti-HIV-1 p24 clone KC57	Beckman Coulter	Cat# 6604667; RRID:AB_1575989
APC Mouse Anti-Human CD45 Clone HI30	BD Biosciences	Cat# 561864; RRID:AB_11153499
FITC Mouse Anti-Human CD3 Clone HIT3a	BD Biosciences	Cat# 555339; RRID:AB_395745
PE Mouse Anti-Human CD8 Clone RPA-T8	Biolegend	Cat# 555367; RRID:AB_395770
PerCP Mouse Anti-human CD4 Clone RPA-T4	Biolegend	Cat# 300527; RRID:AB_893327
Biological samples		

Human PBMCs from HIV-1-infected and uninfected individuals	FRQS AIDS network and New York Blood Bank	N/A
Plasma form HIV-1-infected individuals	FRQS AIDS network	N/A
Chemicals, peptides, and recombinant proteins		
Dulbecco's modified Eagle's medium (DMEM)	Wisent	Cat# 319-005-CL
Gibco™ Roswell Park Memorial Institute 1640 medium (RPMI)	Thermo Fisher Scientific	Cat# 11875-093
Fetal bovine serum (FBS)	VWR	Cat# 97068-085
Penicillin/streptomycin	Wisent	Cat# 450-200-EL
Tris-buffered saline (TBS)	Thermo Fisher Scientific	Cat# BP24711
Bovine Serum Albumin (BSA)	BioShop	Cat# ALB001.100
Tween20	Thermo Fisher Scientific	Cat# BP337-500
Western Lightning Plus-ECL, Enhanced Chemiluminescence Substrate	Perkin Elmer Life Sciences	Cat# NEL105001EA
Phosphate buffered saline (PBS)	Wisent	Cat# 311-010-CL
Lymphocyte separation medium	Wisent	Cat# 305-010-CL
FreeStyle 293F expression medium	ThermoFisher Scientific	Cat# 12338002
ExpiFectamine 293 transfection reagent	ThermoFisher Scientific	Cat# A14525
Passive lysis buffer	Promega	Cat# E1941
Firefly D-Luciferin Free Acid	Prolume	Cat# 306
eBioscience™ Cell proliferation dye eFluor670	Thermo Fisher Scientific	Cat# 65-0840-90
eBioscience™ Cell proliferation dye eFluor450	Thermo Fisher Scientific	Cat# 65-0842-85
LIVE/DEAD Fixable Aqua Dead Cell Stain	Thermo Fisher Scientific	Cat# L34966
Formaldehyde 37%	Thermo Fisher Scientific	Cat# F79-500
Biotininylated recombinant soluble dimeric FcγRIIIa (V^{158}) protein	(Wines et al., 2016)	N/A
CD4 mimetic BNM-III-170	Dr Amos B. Smith III (Chen et al., 2019)	N/A
Dimethyl sulfoxide (DMSO)	Thermo Fisher Scientific	Cat# D1391
Phytohemagglutinin-L (PHA-L)	Sigma	Cat# L2769
Recombinant IL-2 (rIL-2)	NIH AIDS Reagent Program	Cat# 136
Protein A Sepharose CL-4B	Cytiva	Cat # 17096303
Papain-agarose resin	Thermo Fisher Scientific	Cat # 20341
β-mercaptoethanol	Bio-Rad	Cat# #1610710
Acrylamide/Bis-Acrylamide	Thermo Fisher Scientific	Cat# BP1410-1
Sodium dodecyl sulfate (SDS)	Thermo Fisher Scientific	Cat # BP166-500
Ammonium Persulfate	Bio-Rad	Cat# 1610700

TEMED	Bio-Rad	Cat# 1610801
Coomassie Brilliant Blue R-250	Thermo Fisher Scientific	Cat# BP101-50
Magnesium phosphate ($MgSO_4$)	Bioshop	Cat# MAG511.500
Potassium phosphate monobasic (KH_2PO_4)	Thermo Fisher Scientific	Cat# P285-500
Adenosine 5-triphosphate disodium salt hydrate (ATP)	Sigma	Cat# A3377-10G
Dithiothreitol (DTT)	Thermo Fisher Scientific	Cat# BP172-5
HIV-1 Env gp41 peptide (583-618)	(Gohain et al., 2016)	N/A
HIV-1 Env gp41 peptide (587-597)	Genscript	N/A
HIV-1 Env gp41 peptide (596-606)	Genscript	N/A
SARS-CoV-2 Spike S2 peptide (1153-1163)	(Li et al., 2021)	N/A
Critical commercial assays		
QuikChange II XL Site-Directed Mutagenesis Kit	Agilent Technologies	Cat # #200522
Alexa Fluor 647 Protein Labeling Kit	Thermo Fisher Scientific	Cat# A20173
EasySep human CD4+ T cell enrichment kit	StemCell Technologies	Cat# 19052
Cytofix/Cytoperm Fixation/ Permeabilization Kit	BD Biosciences	Cat# 554714
QIAamp viral RNA mini kit	QIAGEN	Cat# 52906
Quantitect SYBR green RT-PCR Master Mix	QIAGEN	Cat# 204245
Experimental models: Cell lines		
293T human embryonic kidney cells	ATCC	Cat# CRL-3216; RRID: CVCL_0063
TZM-bl cells	NIH AIDS Reagent Program	Cat# 8129; RRID:CVCL_B478
FreeStyle 293F cells	Thermo Fisher Scientific	Cat# R79007; RRID: CVCL_D603
Experimental models: Organisms/strains		
SIRPA $^{h/m}$ Rag2$^{-/-}$ Il2rg$^{-/-}$ IL15 $^{h/m}$ (SRG-15) mice	(Herndler-Brandstetter et al., 2017)	N/A
Oligonucleotides		
246D heavy chain G236R FWD: 5'-CCTGAACTCCTGCGGGGACCGTCAGTC-3' REV: 5'-GACTGACGGTCCCCGCAGGAGTTCAGG-3'	Integrated DNA Technologies	N/A
246D heavy chain L328R FWD: 5'-CCAACAAAGCCCGCCCAGCCCCCATC-3' REV: 5'-GATGGGGGCTGGGCGGGCTTTGTTGG-3'	Integrated DNA Technologies	N/A
246D heavy chain G236A/S239D FWD: 5'-CTCCTGGCGGGACCGGATGTCTTCCTCTTC-3' REV: 5'-GAAGAGGAAGACATCCGGTCCCGCCAGGAG-3'	Integrated DNA Technologies	N/A
246D heavy chain A330L/I332E FWD: 5'-GCCCTCCCACTCCCCGAAGAGAAAACCATC-3' REV: 5'-GATGGTTTTCTCTTCGGGGAGTGGGAGGGC-3'	Integrated DNA Technologies	N/A
HIV-1 IMC JR-CSF Vpu- primers FWD:5'-GTGCATGTAATGTAACCTTTACAAATATTAGC-3' REV: 5'-GCTAATATTTGTAAAGGTTACATTACATGCAC-3'	Integrated DNA Technologies	N/A

HIV-$1_{NL4/3}$YU2 Vpu+ primers FWD: 5'-GTAAGTAGTACATGTAATGCAACCTATACC-3' REV: 5'-GGTATAGGTTGCATTACATGTACTACTTAC-3'	Integrated DNA Technologies	N/A
HIV-1 *gag* primers FWD: 5'-TGCTATGTCAGTTCCCCTTGGTTCTCT-3' REV: 5'-AGTTGGAGGACATCAAGCAGCCATGCAAAT-3'	(Rajashekar et al., 2021)	N/A
Recombinant DNA		
246D mAb Light Chain Expression Vector	NIH AIDS Reagent Program	Cat# 13742
246D mAb Heavy Chain Expression Vector	NIH AIDS Reagent Program	Cat# 13741
246D GRLR mAb Heavy Chain Expression Vector	This paper	N/A
246D GASDALIE mAb Heavy Chain Expression Vector	This paper	N/A
HIV-$1_{NL4/3}$YU2	(Horwitz et al., 2017)	N/A
HIV-$1_{NL4/3}$YU2 Vpu+	This paper	N/A
HIV-1 IMC JR-CSF	NIH AIDS Reagent Program (Koyanagi et al., 1987)	Cat# 2708
HIV-1 IMC JR-CSF Vpu-	This paper	N/A
HIV-1 IMC NL4/3	NIH AIDS Reagent Program (Adachi et al., 1986)	Cat# 114
HIV-1 IMC NL4/3 Vpu-	(Neil et al., 2006)	N/A
HIV-1 IMC YU2	(Li et al., 1991)	N/A
HIV-1 IMC YU2 Vpu+	(Krapp et al., 2016)	N/A
HIV-1 IMC AD8	(Theodore et al., 1996)	N/A
HIV-1 IMC AD8 Vpu+	(Krapp et al., 2016)	N/A
HIV-1 IMC CH058	(Ochsenbauer et al., 2012)	N/A
HIV-1 IMC CH058 Vpu-	(Kmiec et al., 2016)	N/A
HIV-1 IMC CH058 Nef-	(Heigele et al., 2016)	N/A
HIV-1 IMC CH058 Nef- Vpu-	(Heigele et al., 2016)	N/A
HIV-1 IMC CH077	(Ochsenbauer et al., 2012)	N/A
HIV-1 IMC CH077 Vpu-	(Kmiec et al., 2016)	N/A
HIV-1 IMC REJO	(Ochsenbauer et al., 2012)	N/A
HIV-1 IMC REJO Vpu-	(Yamada et al., 2018)	N/A
HIV-1 IMC STCO	(Parrish et al., 2013)	N/A
HIV-1 IMC STCO Vpu-	(Kmiec et al., 2016)	N/A
HIV-1 IMC CH198	(Parrish et al., 2013)	N/A
HIV-1 IMC CH198 Vpu-	(Sauter et al., 2015)	N/A
HIV-1 IMC ZM246F	(Parrish et al., 2012)	N/A
HIV-1 IMC ZM246F Vpu-	(Langer et al., 2015)	N/A

HIV-1 IMC CH167	(Parrish et al., 2013)	N/A
HIV-1 IMC CH167 Vpu-	(Kmiec et al., 2016)	N/A
HIV-1 IMC CH293	(Parrish et al., 2013)	N/A
HIV-1 IMC CH293 Vpu-	(Sauter et al., 2015)	N/A
VSV G glycoprotein expression vector	(Emi et al., 1991)	N/A
Software and algorithms		
BD FACSDiva v9.0	BD Biosciences	RRID: SCR_001456
FlowJo v10.5.3	Tree Star	https://www.flowjo.com/; RRID:SCR_008520
GraphPad Prism v9.1.0	GraphPad	https://www.graphpad.com/; RRID:SCR_002798
Other		
BD LSR II Flow Cytometer	BD Biosciences	N/A
TriStar LB 942 Microplate Reader	Berthold Technologies	N/A
Applied Biosystems 7500 real-time PCR system	Thermo Fisher Scientific	N/A
Biacore 3000	Cytiva	RRID: SCR_019954
Protein A sensor chip	Cytiva	Cat # 29127558
Superdex 200 16/60 column	Cytiva	Cat# 17-1069-01
Superdex 200 10/300 GL column	Cytiva	Cat# 17-5175-01
Clear V-bottom 96-well plates (cell culture-treated)	Corning	Cat# 0720096
White flat-bottom 96-well plates (cell culture-treated)	Corning	Cat# 0877126
White Maxisorp™ Nunc™ 96-well plates	Thermo Fisher Scientific	Cat# 437796

RESOURCE AVAILABILITY

Lead Contact

Further information and requests for resources and reagents should be directed to and will be fulfilled by the Lead Contact, Andrés Finzi (andres.finzi@umontreal.ca).

Materials Availability

All unique reagents generated in this study are available from the Lead Contact with a completed Materials Transfer Agreement.

Data and Code Availability

The published article includes all datasets generated and analyzed for this study. Further information and requests for resources and reagents should be directed to and will be fulfilled by the Lead Contact Author (andres.finzi@umontreal.ca).

EXPERIMENTAL MODELS AND SUBJECT DETAILS

Ethics Statement

Written informed consent was obtained from all study participants and research adhered to the ethical guidelines of CRCHUM and was reviewed and approved by the CRCHUM institutional review board (ethics committee, approval number CE 16.164 - CA). Research adhered to the standards indicated by the Declaration of Helsinki. All participants were adult and provided informed written consent prior to enrolment in accordance with Institutional Review Board approval.

Cell lines and primary cells

293T human embryonic kidney cells (obtained from ATCC) and TZM-bl cells (NIH AIDS Reagent Program) were maintained at 37°C under 5% CO_2 in Dulbecco's Modified Eagle Medium (DMEM) (Wisent, St. Bruno, QC, Canada), supplemented with 5% fetal bovine serum (FBS) (VWR, Radnor, PA, USA) and 100 U/mL penicillin/streptomycin (Wisent). 293T cells were derived from 293 cells, into which the simian virus 40 T-antigen was inserted. TZM-bl cells were derived from HeLa cells and were engineered to stably express high levels of human

CD4 and CCR5 and to contain the firefly luciferase reporter gene under the control of the HIV-1 promoter (Platt et al., 1998). Human peripheral blood mononuclear cells (PBMCs) from ten HIV-negative individuals (8 males and 2 females) and five antiretroviral therapy (ART)-treated HIV-positive individuals (all males) obtained by leukapheresis and Ficoll-Paque density gradient isolation were cryopreserved in liquid nitrogen until further use. CD4+ T lymphocytes were purified from resting PBMCs by negative selection using immunomagnetic beads per the manufacturer's instructions (StemCell Technologies, Vancouver, BC) and were activated with phytohemagglutinin-L (10 µg/mL) for 48 h and then maintained in RPMI 1640 (Thermo Fisher Scientific, Waltham, MA, USA) complete medium supplemented with rIL-2 (100 U/mL).

Human plasma samples

The FRQS-AIDS and Infectious Diseases Network supports a representative cohort of newly-HIV-infected subjects with clinical indication of primary infection [the Montreal Primary HIV Infection Cohort (Fontaine et al., 2011; Fontaine et al., 2009)]. Cross-sectional plasma samples from 50 HIV-1-infected individuals were segregated in five groups based on infection duration and treatment with antiretroviral therapy (ART). Plasma samples were obtained from treatment-naive subjects during the acute phase of infection (first 3 months after HIV acquisition), the early phase of infection (3–6 and 6-12 months after acquisition) and during the chronic phase of infection (>2 years after acquisition). Another group of chronically-infected individuals (>2 years after acquisition) received ART treatment. Plasma samples were also obtained from ten age- and sex-matched HIV-negative healthy volunteers.

Experimental animal models

SRG-15 mice encoding human SIRPA and IL-15 in a 129xBALB/c (N3) genetic background were originally generated in the laboratory of Dr Richard Flavell (Yale University) (Herndler-Brandstetter et al., 2017). The mice were bred and maintained under specific pathogen-free conditions. All animal studies were performed with authorization from Institutional Animal Care and Use Committees (IACUC) of Yale University. SRG-15-Hu-PBL mice were engrafted as described (Rajashekar et al., 2021). Briefly, 3.5×10^6 PBMCs, purified by Ficoll density gradient centrifugation of healthy donor blood buffy coats (one male, obtained from the New York Blood Bank) were injected IP in a 200-µL volume into 6- to 8-week-old SRG-15 mice, using a 1-cm^3 syringe and 25-gauge needle. Cell engraftment was tested 15 days post-transplant. 100 µL of blood was collected by retroorbital bleeding. PBMCs were isolated by Ficoll density gradient centrifugation; stained with fluorescently-labelled anti-human CD45, CD3, CD4, CD8 and CD56 antibodies and analyzed by flow cytometry to confirm engraftment. Humanized mice were intraperitoneally challenged with 30,000 PFU of HIV-$1_{NL4/3}$YU2 Vpu- or Vpu+. Infection profile was analyzed through routinely by retro-orbital bleeds for plasma viral load (PVL) analysis.

METHOD DETAILS

Plasmids and proviral constructs

The HIV-$1_{NL4/3}$YU2 proviral construct has been previously reported (Horwitz et al., 2017). A mutation was introduced in the putative *vpu* start codon (ACG → ATG) to restore the *vpu* open reading frame (ORF) in the HIV-$1_{NL4/3}$YU2 IMC using the QuikChange II XL site-directed mutagenesis protocol (Agilent Technologies, Santa Clara, CA). Transmitted/Founder (T/F) and chronic infectious molecular clones (IMCs) of patients CH058, CH077, CH198, ZM246F,

659 CH167, CH293, REJO, STCO were inferred and constructed as previously described
660 (Ochsenbauer et al., 2012; Parrish et al., 2013; Parrish et al., 2012; Salazar-Gonzalez et al.,
661 2009). The generation of *vpu*-defective IMCs was previously described (Kmiec et al., 2016;
662 Langer et al., 2015; Sauter et al., 2015; Yamada et al., 2018) and consists in the introduction of
663 premature stop codons in the *vpu* reading frame using the QuikChange II XL site-directed
664 mutagenesis protocol. CH058 IMCs defective for Vpu and/or Nef expression were previously
665 described (Heigele et al., 2016; Kmiec et al., 2016). The IMCs encoding for HIV-1 reference
666 strains NL4/3, AD8, YU2 and JR-CSF were described elsewhere (Adachi et al., 1986; Koyanagi
667 et al., 1987; Krapp et al., 2016; Li et al., 1991; Theodore et al., 1996). To generate *vpu*-defective
668 JR-CSF IMC, a stop-codon was introduced directly after the start-codon of *vpu* using the
669 QuikChange II XL site-directed mutagenesis protocol. The plasmids encoding for the heavy and
670 light chains of the 246D antibody are available through the NIH AIDS Reagent Program. Site-
671 directed mutagenesis was performed on the plasmid expressing 246D antibody heavy chain to
672 introduce the GRLR mutations (G236R/L328R) or the GASDALIE mutations
673 (G236A/S239D/A330L/I332E) using the QuikChange II XL site-directed mutagenesis protocol.
674 The presence of the desired mutations was determined by automated DNA sequencing. The
675 vesicular stomatitis virus G (VSV-G)-encoding plasmid was previously described (Emi et al.,
676 1991).
677
678 **Viral production, infections and *ex vivo* amplification.**
679 For *in vitro* infection, vesicular stomatitis virus G (VSV-G)-pseudotyped HIV-1 viruses were
680 produced by co-transfection of 293T cells with an HIV-1 proviral construct and a VSV-G-
681 encoding vector using the calcium phosphate method. Two days post-transfection, cell

682 supernatants were harvested, clarified by low-speed centrifugation (300 × g for 5 min), and
683 concentrated by ultracentrifugation at 4°C (100,605 × g for 1 h) over a 20% sucrose cushion.
684 Pellets were resuspended in fresh RPMI, and aliquots were stored at −80°C until use. Viruses
685 were then used to infect activated primary CD4+ T cells from healthy HIV-1 negative donors by
686 spin infection at 800 × *g* for 1 h in 96-well plates at 25 °C. Viral preparations were titrated
687 directly on primary CD4+ T cells to achieve similar levels of infection among the different
688 IMCs tested (around 10% of p24+ cells). To expand endogenously infected CD4+ T cells,
689 primary CD4+ T cells obtained from ART-treated HIV-1-infected individuals were isolated
690 from PBMCs by negative selection. Purified CD4+ T cells were activated with PHA-L at
691 10 µg/mL for 48 h and then cultured for at least 6 days in RPMI 1640 complete medium
692 supplemented with rIL-2 (100 U/ml) to reach greater than 10% infection for the ADCC assay.
693
694 **Antibodies**
695 The following Abs were used to assess cell-surface Env staining: anti-gp41 nnAbs QA255-006,
696 QA255-067, QA255-072 (kindly provided by Julie Overbaugh), 7B2, 2.2B, 12.3D, 12.4H
697 (kindly provided by James Robinson), F240 (NIH AIDS Reagent Program), M785U1, M785U2,
698 M785U3, M785U4, N10U1, N10U2, N5U1, N5U2, N5U3 (kindly provided by George Lewis),
699 246D, 240D, 167D, and 50-69; anti-cluster A A32 (NIH AIDS Reagent Program), C11 (kindly
700 provided by James Robinson) and N5i5; anti-co-receptor binding site 17b (NIH AIDS Reagent
701 Program) and X5; anti-V3 loop GE2-JG8 (kindly provided by Gunilla Karlsson Hedestam); anti-
702 CD4 binding site VRC01, VRC03, VRC07-523, VRC13, VRC16 (kindly provided by John
703 Mascola), N6 (kindly provided by Mark Connors), 1-18 (kindly provided by Florian Klein),
704 HJ16, CH106 (NIH AIDS Reagent Program), NC-Cow1, b12, 3BNC117 and N49-P7; anti-V3

glycan PGT121, PGT122, PGT123, PGT125, PGT126, PGT128, PGT130, PGT135, PGT136 (IAVI), BG18 and 10-1074; anti-V2 apex PGT145, PG9 and PG16 (IAVI); anti-gp120-gp41 interface PGT151 (IAVI), 35O22 (kindly provided by Mark Connors), VRC34 (kindly provided by John Mascola) and 8ANC195; anti-silent face SF12; anti-MPER 10E8 (kindly provided by Mark Connors), 4E10 and 2F5 (NIH AIDS Reagent Program). The HIV-IG polyclonal antibody consists of anti-HIV immunoglobulins purified from a pool of plasma from HIV+ asymptomatic donors (NIH AIDS Reagent Program). Mouse anti-human CD4 (clone OKT4; Thermo Fisher Scientific), mouse anti-human BST-2 (clone RS38E, PE-Cy7-conjugated; Biolegend, San Diego, CA, USA), mouse anti-human NTB-A (clone NT-7, Biolegend) and mouse anti-PVR (clone SKII.4, Biolegend) were also used as primary antibodies for cell-surface staining. Goat anti-mouse IgG (H+L), goat anti-human IgG (H+L) (Thermo Fisher Scientific) and mouse anti-human IgG Fc (Biolegend) antibodies pre-coupled to Alexa Fluor 647 were used as secondary antibodies in flow cytometry experiments. Rabbit antisera raised against Nef (NIH AIDS Reagent Program) or Vpu (Prevost et al., 2020a) were used as primary antibodies in intracellular staining. BrillantViolet 421 (BV421)-conjugated donkey anti-rabbit antibodies (Biolegend) were used as secondary antibodies to detect Nef and Vpu antisera binding by flow cytometry. Goat anti-human IgG Fc antibodies conjugated to horseradish peroxidase (HRP; Thermo Fisher Scientific) were used as secondary antibodies in ELISA experiments.

Small CD4-mimetics

The small-molecule CD4-mimetic compound (CD4mc) BNM-III-170 was synthesized as described previously (Chen et al., 2019). The compounds were dissolved in dimethyl sulfoxide

(DMSO) at a stock concentration of 10 mM and diluted to 50 µM in phosphate-buffered saline (PBS) for cell-surface staining or in RPMI-1640 complete medium for ADCC assays.

Protein production of recombinant proteins

FreeStyle 293F cells (Thermo Fisher Scientific) were grown in FreeStyle 293F medium (Thermo Fisher Scientific) to a density of 1×10^6 cells/ml at 37 °C with 8 % CO_2 with regular agitation (150 rpm). Cells were transfected with plasmids expressing the light and heavy chains of a given antibody using ExpiFectamine 293 transfection reagent, as directed by the manufacturer (Thermo Fisher Scientific). One week later, the cells were pelleted and discarded. The supernatants were filtered (0.22-µm-pore-size filter), and antibodies were purified by protein A affinity columns, as directed by the manufacturer (Cytiva, Marlborough, MA, USA). The recombinant protein preparations were dialyzed against phosphate-buffered saline (PBS) and stored in aliquots at −80°C. To assess purity, recombinant proteins were loaded on SDS-PAGE polyacrylamide gels in the presence or absence of β-mercaptoethanol and stained with Coomassie blue. Purified F240 and 2.2B IgG were conjugated with Alexa Fluor 647 dye according to the manufacturer's protocol (Thermo Fisher Scientific). The F240 Fab fragments were prepared from purified IgG (10 mg/mL) by proteolytic digestion with immobilized papain (Pierce, Rockford, IL) and purified using protein A, followed by gel filtration chromatography on a Superdex 200 16/60 column (Cytiva). The biotin-tagged dimeric recombinant soluble FcγRIIIa (V^{158}) protein was produced and characterized as described (Wines et al., 2016) with additional purification step using a Superdex 200 10/300 GL column (Cytiva).

Flow cytometry analysis of cell-surface staining

Cell surface staining was performed at 48h post-infection. Mock-infected or HIV-1-infected primary CD4+ T cells were incubated for 30 min at 37°C with anti-CD4 (0.5 µg/mL), anti-BST-2 (2 µg/mL), anti-NTB-A (5 µg/mL), anti-PVR (10 µg/mL), anti-Env mAbs (5 µg/mL), HIV-IG (50 µg/mL) or plasma (1:1000 dilution). Cells were then washed once with PBS and stained with the appropriate Alexa Fluor 647-conjugated secondary antibody (2 µg/mL), when needed, for 20 min at room temperature. After one more PBS wash, cells were fixed in a 2% PBS-formaldehyde solution. Alternatively, the binding of anti-Env Abs was detected using a biotin-tagged dimeric recombinant soluble FcγRIIIa (0.2 µg/mL) followed by the addition of Alexa Fluor 647-conjugated streptavidin (Thermo Fisher Scientific; 2 µg/mL). Anti-human IgG Fc secondary antibodies (3 µg/mL) were used when cell surface binding was performed in presence of F240 Fab blockade. Infected cells were then permeabilized using the Cytofix/Cytoperm Fixation/ Permeabilization Kit (BD Biosciences, Mississauga, ON, Canada) and stained intracellularly using PE-conjugated mouse anti-p24 mAb (clone KC57; Beckman Coulter, Brea, CA, USA; 1:100 dilution) in combination with Nef or Vpu rabbit antisera (1:1000 dilution). The percentage of infected cells ($p24^+$) was determined by gating on the living cell population according to a viability dye staining (Aqua Vivid; Thermo Fisher Scientific). Alternatively, cells were stained intracellularly with rabbit antisera raised against Nef or Vpu (1:1000) followed by BV421-conjugated anti-rabbit secondary antibody. Samples were acquired on an LSR II cytometer (BD Biosciences), and data analysis was performed using FlowJo v10.5.3 (Tree Star, Ashland, OR, USA).

Antibody-dependant cellular cytotoxicity (ADCC) assay

Measurement of ADCC using a fluorescence-activated cell sorting (FACS)-based infected cell

elimination (ICE) assay was performed at 48 h post-infection. Briefly, HIV-1-infected primary CD4+ T cells were stained with AquaVivid viability dye and cell proliferation dye eFluor670 (Thermo Fisher Scientific) and used as target cells. Cryopreserved autologous PBMC effectors cells, stained with cell proliferation dye eFluor450 (Thermo Fisher Scientific), were added at an effector: target ratio of 10:1 in 96-well V-bottom plates (Corning, Corning, NY). A 1:1000 final dilution of plasma or 5 µg/mL of anti-Env mAbs was added to appropriate wells and cells were incubated for 5 min at room temperature. The plates were subsequently centrifuged for 1 min at 300 × g, and incubated at 37 °C, 5 % CO_2 for 5 h before being fixed in a 2 % PBS-formaldehyde solution. Infected cells were identified by intracellular p24 staining as described above. Samples were acquired on an LSR II cytometer (BD Biosciences) and data analysis was performed using FlowJo v10.5.3 (Tree Star). The percentage of ADCC was calculated with the following formula: [(% of p24+ cells in Targets plus Effectors) − (% of p24+ cells in Targets plus Effectors plus plasma) / (% of p24+ cells in Targets) × 100] by gating on infected lived target cells.

Virus neutralization assay

TZM-bl target cells were seeded at a density of 2×10^4 cells/well in 96-well luminometer-compatible tissue culture plates (PerkinElmer, Waltham, MA, USA) 24 h before infection. HIV-$1_{NL4/3}$YU2 Vpu- or Vpu+ (in a final volume of 50 µl) was pre-incubated with the indicated amounts of mAbs for 1 h at 37 °C before adding to the target cells. Following an incubation of 24 h at 37 °C, 100 µl of media was added to each well. Two days later, the medium was removed from each well, and the cells were lysed by the addition of 30 µl of passive lysis buffer (Promega, Madison, WI, USA) followed by one freeze-thaw cycle. An LB 942 TriStar luminometer (Berthold Technologies, Bad Wildbad, Germany) was used to measure the

luciferase activity in each well after the addition of 100 µL of Luciferin buffer (15 mM $MgSO_4$, 15 mM KH_2PO_4 [pH 7.8], 1 mM ATP, and 1 mM dithiothreitol) and 50 µL of 1 mM Firefly D-luciferin (Prolume, Pinetop, AZ, USA).

Plasma viral load measurements

Quantification of PVLs was done using the method described previously (Gibellini et al., 2004). Briefly, 100 µL of blood was collected from mice at each time point by retroorbital bleed. Plasma viral RNA was extracted using the QIAamp viral RNA mini kit (QIAGEN, Hilden Germany) following the manufacturer's protocol. SYBR green real-time PCR assay was carried out in a 20-µL PCR mixture volume consisting of 10 µL of 2× Quantitect SYBR green RT-PCR Master Mix (QIAGEN) containing HotStarTaq DNA polymerase, 0.5 µL of 500 nM each oligonucleotide primer, 0.2 µL of 100× QuantiTect RT Mix (containing Omniscript and Sensiscript RTs), and 8 µL of RNA extracted from plasma samples or standard HIV-1 RNA (from 5×10^5 to 5 copies per 1 mL). Highly conserved sequences on the gag region of HIV-1 were chosen, and specific HIV-1 gag primers were selected. The sequences of HIV-1 gag primers are 5' TGCTATGTCAGTTCCCCTTGGTTCTCT 3' and 5'AGTTGGAGGACATCAAGCAGCCATGCAAAT 3'. Amplification was done in an Applied Biosystems 7500 real-time PCR system, and it involved activation at 45 °C for 15 min and 95 °C for 15 min followed by 40 amplification cycles of 95 °C for 15 s, 60 °C for 15 s, and 72 °C for 30 s. For the detection and quantification of viral RNA, the real-time PCR of each sample was compared with threshold cycle value of a standard curve.

Sequence analysis

The LOGO plot (Crooks et al., 2004) was created using the Analyze Align tool at the Los Alamos National Laboratory - HIV database which is based on the WebLogo program (https://www.hiv.lanl.gov/content/sequence/ANALYZEALIGN/analyze_align.html) and the HIV-1 database global curated and filtered 2019 alignment, including 6,223 individual Env protein sequences. The relative height of each letter within individual stack represents the frequency of the indicated amino acid at that position. The numbering of Env amino acid sequences is based on the HXB2 reference strain of HIV-1, where 1 is the initial methionine.

gp41 peptide ELISA

Peptides corresponding to the gp41 C-C loop region (residues 583-618) were either previously described (Gohain et al., 2016) or purchased from Genscript (Piscataway, NJ, USA). A peptide corresponding to the SARS-CoV-2 Spike S2 stem helix (residues 1153-1163) was used as a negative control and was previously reported (Li et al., 2021). Peptides were prepared in PBS at a concentration of 1 µg/mL and were adsorbed to white 96-well plates (MaxiSorp Nunc) overnight at 4 °C. Coated wells were subsequently blocked with blocking buffer (Tris buffered saline [TBS] containing 0.1% Tween20 and 2% BSA) for 1 hour at room temperature. Wells were then washed four times with washing buffer (TBS containing 0.1% Tween20). Anti-gp41 246D and F240 or anti-gp120 A32 (50 ng/mL) were prepared in a diluted solution of blocking buffer (0.1 % BSA) and incubated with the peptide-coated wells for 90 minutes at room temperature. Plates were washed four times with washing buffer followed by incubation with horseradish peroxidase (HRP)-conjugated anti-human IgG secondary Ab (0.3 µg/mL in a diluted solution of blocking buffer [0.4% BSA]) for 1 h at room temperature, followed by four washes. HRP enzyme activity was determined after the addition of a 1:1 mix of Western Lightning Plus-

ECL oxidizing and luminol reagents (Perkin Elmer Life Sciences). Light emission was measured with a LB942 TriStar luminometer (Berthold Technologies).

Surface plasmon resonance (SPR)

Surface plasmon resonance assays were performed on a Biacore 3000 (Cytiva) with a running buffer of 10 mM HEPES pH 7.5 and 150 mM NaCl, supplemented with 0.05% Tween20 at 25°C. The binding kinetics between the gp41 C-C loop and the 246D antibody were obtained in a format where 246D IgG was immobilized onto a Protein A sensor chip (Cytiva) with ~300 response units (RU) and serial dilutions of gp41 (583-618) synthetic peptide were injected with concentrations ranging from 0.488 to 31.25 nM. The protein A chip was regenerated with a wash step of 0.1 M glycine pH 2.0 and reloaded with IgG after each cycle. Kinetic constants were determined using a 1:1 Langmuir model in bimolecular interaction analysis (BIA) evaluation software.

QUANTIFICATION AND STATISTICAL ANALYSIS

Statistics were analyzed using GraphPad Prism version 9.1.0 (GraphPad, San Diego, CA, USA). Every data set was tested for statistical normality and this information was used to apply the appropriate (parametric or nonparametric) statistical test. P values <0.05 were considered significant; significance values are indicated as * $P<0.05$, ** $P<0.01$, *** $P<0.001$, **** $P<0.0001$.

REFERENCES

Acharya, P., Tolbert, W.D., Gohain, N., Wu, X., Yu, L., Liu, T., Huang, W., Huang, C.C., Kwon, Y.D., Louder, R.K., *et al.* (2014). Structural Definition of an Antibody-Dependent Cellular Cytotoxicity Response Implicated in Reduced Risk for HIV-1 Infection. J Virol *88*, 12895-12906.

Adachi, A., Gendelman, H.E., Koenig, S., Folks, T., Willey, R., Rabson, A., and Martin, M.A. (1986). Production of acquired immunodeficiency syndrome-associated retrovirus in human and nonhuman cells transfected with an infectious molecular clone. J Virol *59*, 284-291.

Alsahafi, N., Bakouche, N., Kazemi, M., Richard, J., Ding, S., Bhattacharyya, S., Das, D., Anand, S.P., Prevost, J., Tolbert, W.D., *et al.* (2019). An Asymmetric Opening of HIV-1 Envelope Mediates Antibody-Dependent Cellular Cytotoxicity. Cell Host Microbe *25*, 578-587 e575.

Alsahafi, N., Ding, S., Richard, J., Markle, T., Brassard, N., Walker, B., Lewis, G.K., Kaufmann, D.E., Brockman, M.A., and Finzi, A. (2016). Nef Proteins from HIV-1 Elite Controllers Are Inefficient at Preventing Antibody-Dependent Cellular Cytotoxicity. J Virol *90*, 2993-3002.

Alvarez, R.A., Hamlin, R.E., Monroe, A., Moldt, B., Hotta, M.T., Rodriguez Caprio, G., Fierer, D.S., Simon, V., and Chen, B.K. (2014). HIV-1 Vpu antagonism of tetherin inhibits antibody-dependent cellular cytotoxic responses by natural killer cells. J Virol *88*, 6031-6046.

Anand, S.P., Prevost, J., Baril, S., Richard, J., Medjahed, H., Chapleau, J.P., Tolbert, W.D., Kirk, S., Smith, A.B., III, Wines, B.D., *et al.* (2019). Two Families of Env Antibodies Efficiently Engage Fc-Gamma Receptors and Eliminate HIV-1-Infected Cells. J Virol *93*.

Arias, J.F., Heyer, L.N., von Bredow, B., Weisgrau, K.L., Moldt, B., Burton, D.R., Rakasz, E.G., and Evans, D.T. (2014). Tetherin antagonism by Vpu protects HIV-infected cells from antibody-dependent cell-mediated cytotoxicity. Proc Natl Acad Sci U S A *111*, 6425-6430.

Asokan, M., Dias, J., Liu, C., Maximova, A., Ernste, K., Pegu, A., McKee, K., Shi, W., Chen, X., Almasri, C., *et al.* (2020). Fc-mediated effector function contributes to the in vivo antiviral effect of an HIV neutralizing antibody. Proc Natl Acad Sci U S A *117*, 18754-18763.

Bar, K.J., Sneller, M.C., Harrison, L.J., Justement, J.S., Overton, E.T., Petrone, M.E., Salantes, D.B., Seamon, C.A., Scheinfeld, B., Kwan, R.W., *et al.* (2016). Effect of HIV Antibody VRC01 on Viral Rebound after Treatment Interruption. N Engl J Med *375*, 2037-2050.

Barouch, D.H., Whitney, J.B., Moldt, B., Klein, F., Oliveira, T.Y., Liu, J., Stephenson, K.E., Chang, H.W., Shekhar, K., Gupta, S., *et al.* (2013). Therapeutic efficacy of potent neutralizing HIV-1-specific monoclonal antibodies in SHIV-infected rhesus monkeys. Nature *503*, 224-228.

Beaudoin-Bussieres, G., Prevost, J., Gendron-Lepage, G., Melillo, B., Chen, J., Smith Iii, A.B., Pazgier, M., and Finzi, A. (2020). Elicitation of Cluster A and Co-Receptor Binding Site Antibodies are Required to Eliminate HIV-1 Infected Cells. Microorganisms *8*.

Bolton, D.L., Pegu, A., Wang, K., McGinnis, K., Nason, M., Foulds, K., Letukas, V., Schmidt, S.D., Chen, X., Todd, J.P., *et al.* (2016). Human Immunodeficiency Virus Type 1 Monoclonal Antibodies Suppress Acute Simian-Human Immunodeficiency Virus Viremia and Limit Seeding of Cell-Associated Viral Reservoirs. J Virol *90*, 1321-1332.

Bour, S., Perrin, C., and Strebel, K. (1999). Cell surface CD4 inhibits HIV-1 particle release by interfering with Vpu activity. J Biol Chem *274*, 33800-33806.

Bournazos, S., Gazumyan, A., Seaman, M.S., Nussenzweig, M.C., and Ravetch, J.V. (2016). Bispecific Anti-HIV-1 Antibodies with Enhanced Breadth and Potency. Cell *165*, 1609-1620.

907 Bournazos, S., Klein, F., Pietzsch, J., Seaman, M.S., Nussenzweig, M.C., and Ravetch, J.V.
908 (2014). Broadly neutralizing anti-HIV-1 antibodies require Fc effector functions for in vivo
909 activity. Cell *158*, 1243-1253.
910 Bruel, T., Guivel-Benhassine, F., Lorin, V., Lortat-Jacob, H., Baleux, F., Bourdic, K., Noel, N.,
911 Lambotte, O., Mouquet, H., and Schwartz, O. (2017). Lack of ADCC breadth of human non-
912 neutralizing anti-HIV-1 antibodies. J Virol.
913 Buchacher, A., Predl, R., Strutzenberger, K., Steinfellner, W., Trkola, A., Purtscher, M., Gruber,
914 G., Tauer, C., Steindl, F., Jungbauer, A., and et al. (1994). Generation of human monoclonal
915 antibodies against HIV-1 proteins; electrofusion and Epstein-Barr virus transformation for
916 peripheral blood lymphocyte immortalization. AIDS Res Hum Retroviruses *10*, 359-369.
917 Burton, D.R., Hessell, A.J., Keele, B.F., Klasse, P.J., Ketas, T.A., Moldt, B., Dunlop, D.C.,
918 Poignard, P., Doyle, L.A., Cavacini, L.*, et al.* (2011). Limited or no protection by weakly or
919 nonneutralizing antibodies against vaginal SHIV challenge of macaques compared with a
920 strongly neutralizing antibody. Proc Natl Acad Sci U S A *108*, 11181-11186.
921 Burton, D.R., Pyati, J., Koduri, R., Sharp, S.J., Thornton, G.B., Parren, P.W., Sawyer, L.S.,
922 Hendry, R.M., Dunlop, N., Nara, P.L., and et al. (1994). Efficient neutralization of primary
923 isolates of HIV-1 by a recombinant human monoclonal antibody. Science *266*, 1024-1027.
924 Caskey, M., Klein, F., Lorenzi, J.C., Seaman, M.S., West, A.P., Jr., Buckley, N., Kremer, G.,
925 Nogueira, L., Braunschweig, M., Scheid, J.F.*, et al.* (2015). Viraemia suppressed in HIV-1-
926 infected humans by broadly neutralizing antibody 3BNC117. Nature *522*, 487-491.
927 Caskey, M., Schoofs, T., Gruell, H., Settler, A., Karagounis, T., Kreider, E.F., Murrell, B.,
928 Pfeifer, N., Nogueira, L., Oliveira, T.Y.*, et al.* (2017). Antibody 10-1074 suppresses viremia in
929 HIV-1-infected individuals. Nat Med *23*, 185-191.
930 Cavacini, L.A., Emes, C.L., Wisnewski, A.V., Power, J., Lewis, G., Montefiori, D., and Posner,
931 M.R. (1998). Functional and molecular characterization of human monoclonal antibody reactive
932 with the immunodominant region of HIV type 1 glycoprotein 41. AIDS Res Hum Retroviruses
933 *14*, 1271-1280.
934 Chan, D.C., Fass, D., Berger, J.M., and Kim, P.S. (1997). Core structure of gp41 from the HIV
935 envelope glycoprotein. Cell *89*, 263-273.
936 Chen, J., Park, J., Kirk, S.M., Chen, H.C., Li, X., Lippincott, D.J., Melillo, B., and Smith, A.B.,
937 III (2019). Development of an Effective Scalable Enantioselective Synthesis of the HIV-1 Entry
938 Inhibitor BNM-III-170 as the Bis-Trifluoroacetate Salt. Org Process Res Dev *23*, 2464-2469.
939 Corti, D., Langedijk, J.P., Hinz, A., Seaman, M.S., Vanzetta, F., Fernandez-Rodriguez, B.M.,
940 Silacci, C., Pinna, D., Jarrossay, D., Balla-Jhagjhoorsingh, S.*, et al.* (2010). Analysis of memory
941 B cell responses and isolation of novel monoclonal antibodies with neutralizing breadth from
942 HIV-1-infected individuals. PLoS One *5*, e8805.
943 Crooks, G.E., Hon, G., Chandonia, J.M., and Brenner, S.E. (2004). WebLogo: a sequence logo
944 generator. Genome Res *14*, 1188-1190.
945 Dave, V.P., Hajjar, F., Dieng, M.M., Haddad, E., and Cohen, E.A. (2013). Efficient BST2
946 antagonism by Vpu is critical for early HIV-1 dissemination in humanized mice. Retrovirology
947 *10*, 128.
948 Davis, K.L., Gray, E.S., Moore, P.L., Decker, J.M., Salomon, A., Montefiori, D.C., Graham,
949 B.S., Keefer, M.C., Pinter, A., Morris, L.*, et al.* (2009). High titer HIV-1 V3-specific antibodies
950 with broad reactivity but low neutralizing potency in acute infection and following vaccination.
951 Virology *387*, 414-426.

Decker, J.M., Bibollet-Ruche, F., Wei, X., Wang, S., Levy, D.N., Wang, W., Delaporte, E., Peeters, M., Derdeyn, C.A., Allen, S., *et al.* (2005). Antigenic conservation and immunogenicity of the HIV coreceptor binding site. J Exp Med *201*, 1407-1419.

Ding, S., Gasser, R., Gendron-Lepage, G., Medjahed, H., Tolbert, W.D., Sodroski, J., Pazgier, M., and Finzi, A. (2019a). CD4 Incorporation into HIV-1 Viral Particles Exposes Envelope Epitopes Recognized by CD4-Induced Antibodies. J Virol *93*.

Ding, S., Grenier, M.C., Tolbert, W.D., Vezina, D., Sherburn, R., Richard, J., Prevost, J., Chapleau, J.P., Gendron-Lepage, G., Medjahed, H., *et al.* (2019b). A New Family of Small-Molecule CD4-Mimetic Compounds Contacts Highly Conserved Aspartic Acid 368 of HIV-1 gp120 and Mediates Antibody-Dependent Cellular Cytotoxicity. J Virol *93*.

Ding, S., Veillette, M., Coutu, M., Prevost, J., Scharf, L., Bjorkman, P.J., Ferrari, G., Robinson, J.E., Sturzel, C., Hahn, B.H., *et al.* (2016a). A Highly Conserved Residue of the HIV-1 gp120 Inner Domain Is Important for Antibody-Dependent Cellular Cytotoxicity Responses Mediated by Anti-cluster A Antibodies. J Virol *90*, 2127-2134.

Ding, S., Verly, M.M., Princiotto, A., Melillo, B., Moody, T., Bradley, T., Easterhoff, D., Roger, M., Hahn, B.H., Madani, N., *et al.* (2016b). Small Molecule CD4-Mimetics Sensitize HIV-1-infected Cells to ADCC by Antibodies Elicited by Multiple Envelope Glycoprotein Immunogens in Non-Human Primates. AIDS Res Hum Retroviruses.

Diskin, R., Klein, F., Horwitz, J.A., Halper-Stromberg, A., Sather, D.N., Marcovecchio, P.M., Lee, T., West, A.P., Jr., Gao, H., Seaman, M.S., *et al.* (2013). Restricting HIV-1 pathways for escape using rationally designed anti-HIV-1 antibodies. J Exp Med *210*, 1235-1249.

Doores, K.J. (2015). The HIV glycan shield as a target for broadly neutralizing antibodies. FEBS J *282*, 4679-4691.

Dosenovic, P., von Boehmer, L., Escolano, A., Jardine, J., Freund, N.T., Gitlin, A.D., McGuire, A.T., Kulp, D.W., Oliveira, T., Scharf, L., *et al.* (2015). Immunization for HIV-1 Broadly Neutralizing Antibodies in Human Ig Knockin Mice. Cell *161*, 1505-1515.

Dube, M., Bego, M.G., Paquay, C., and Cohen, E.A. (2010). Modulation of HIV-1-host interaction: role of the Vpu accessory protein. Retrovirology *7*, 114.

Dufloo, J., Guivel-Benhassine, F., Buchrieser, J., Lorin, V., Grzelak, L., Dupouy, E., Mestrallet, G., Bourdic, K., Lambotte, O., Mouquet, H., *et al.* (2020). Anti-HIV-1 antibodies trigger non-lytic complement deposition on infected cells. EMBO Rep *21*, e49351.

Earl, P.L., Doms, R.W., and Moss, B. (1990). Oligomeric structure of the human immunodeficiency virus type 1 envelope glycoprotein. Proc Natl Acad Sci U S A *87*, 648-652.

Eda, Y., Murakami, T., Ami, Y., Nakasone, T., Takizawa, M., Someya, K., Kaizu, M., Izumi, Y., Yoshino, N., Matsushita, S., *et al.* (2006). Anti-V3 humanized antibody KD-247 effectively suppresses ex vivo generation of human immunodeficiency virus type 1 and affords sterile protection of monkeys against a heterologous simian/human immunodeficiency virus infection. J Virol *80*, 5563-5570.

Emi, N., Friedmann, T., and Yee, J.K. (1991). Pseudotype formation of murine leukemia virus with the G protein of vesicular stomatitis virus. J Virol *65*, 1202-1207.

Escolano, A., Steichen, J.M., Dosenovic, P., Kulp, D.W., Golijanin, J., Sok, D., Freund, N.T., Gitlin, A.D., Oliveira, T., Araki, T., *et al.* (2016). Sequential Immunization Elicits Broadly Neutralizing Anti-HIV-1 Antibodies in Ig Knockin Mice. Cell *166*, 1445-1458 e1412.

Falkowska, E., Le, K.M., Ramos, A., Doores, K.J., Lee, J.H., Blattner, C., Ramirez, A., Derking, R., van Gils, M.J., Liang, C.H., *et al.* (2014). Broadly neutralizing HIV antibodies define a

997 glycan-dependent epitope on the prefusion conformation of gp41 on cleaved envelope trimers.
998 Immunity *40*, 657-668.
999 Fontaine, J., Chagnon-Choquet, J., Valcke, H.S., Poudrier, J., and Roger, M. (2011). High
1000 expression levels of B lymphocyte stimulator (BLyS) by dendritic cells correlate with HIV-
1001 related B-cell disease progression in humans. Blood *117*, 145-155.
1002 Fontaine, J., Coutlee, F., Tremblay, C., Routy, J.P., Poudrier, J., and Roger, M. (2009). HIV
1003 infection affects blood myeloid dendritic cells after successful therapy and despite
1004 nonprogressing clinical disease. J Infect Dis *199*, 1007-1018.
1005 Freed, E.O., Myers, D.J., and Risser, R. (1989). Mutational analysis of the cleavage sequence of
1006 the human immunodeficiency virus type 1 envelope glycoprotein precursor gp160. J Virol *63*,
1007 4670-4675.
1008 Freund, N.T., Horwitz, J.A., Nogueira, L., Sievers, S.A., Scharf, L., Scheid, J.F., Gazumyan, A.,
1009 Liu, C., Velinzon, K., Goldenthal, A.*, et al.* (2015). A New Glycan-Dependent CD4-Binding Site
1010 Neutralizing Antibody Exerts Pressure on HIV-1 In Vivo. PLoS Pathog *11*, e1005238.
1011 Freund, N.T., Wang, H., Scharf, L., Nogueira, L., Horwitz, J.A., Bar-On, Y., Golijanin, J.,
1012 Sievers, S.A., Sok, D., Cai, H.*, et al.* (2017). Coexistence of potent HIV-1 broadly neutralizing
1013 antibodies and antibody-sensitive viruses in a viremic controller. Sci Transl Med *9*.
1014 Frey, G., Chen, J., Rits-Volloch, S., Freeman, M.M., Zolla-Pazner, S., and Chen, B. (2010).
1015 Distinct conformational states of HIV-1 gp41 are recognized by neutralizing and non-
1016 neutralizing antibodies. Nat Struct Mol Biol *17*, 1486-1491.
1017 Fritschi, C.J., Liang, S., Mohammadi, M., Anang, S., Moraca, F., Chen, J., Madani, N., Sodroski,
1018 J.G., Abrams, C.F., Hendrickson, W.A., and Smith, A.B., 3rd (2021). Identification of gp120
1019 Residue His105 as a Novel Target for HIV-1 Neutralization by Small-Molecule CD4-Mimics.
1020 ACS Med Chem Lett *12*, 1824-1831.
1021 Gibellini, D., Vitone, F., Gori, E., La Placa, M., and Re, M.C. (2004). Quantitative detection of
1022 human immunodeficiency virus type 1 (HIV-1) viral load by SYBR green real-time RT-PCR
1023 technique in HIV-1 seropositive patients. J Virol Methods *115*, 183-189.
1024 Gohain, N., Tolbert, W.D., Orlandi, C., Richard, J., Ding, S., Chen, X., Bonsor, D.A., Sundberg,
1025 E.J., Lu, W., Ray, K.*, et al.* (2016). Molecular basis for epitope recognition by non-neutralizing
1026 anti-gp41 antibody F240. Sci Rep *6*, 36685.
1027 Gorny, M.K., Gianakakos, V., Sharpe, S., and Zolla-Pazner, S. (1989). Generation of human
1028 monoclonal antibodies to human immunodeficiency virus. Proc Natl Acad Sci U S A *86*, 1624-
1029 1628.
1030 Guan, Y., Pazgier, M., Sajadi, M.M., Kamin-Lewis, R., Al-Darmarki, S., Flinko, R., Lovo, E.,
1031 Wu, X., Robinson, J.E., Seaman, M.S.*, et al.* (2013). Diverse specificity and effector function
1032 among human antibodies to HIV-1 envelope glycoprotein epitopes exposed by CD4 binding.
1033 Proc Natl Acad Sci U S A *110*, E69-78.
1034 Halper-Stromberg, A., Lu, C.L., Klein, F., Horwitz, J.A., Bournazos, S., Nogueira, L.,
1035 Eisenreich, T.R., Liu, C., Gazumyan, A., Schaefer, U.*, et al.* (2014). Broadly neutralizing
1036 antibodies and viral inducers decrease rebound from HIV-1 latent reservoirs in humanized mice.
1037 Cell *158*, 989-999.
1038 Haynes, B.F., Gilbert, P.B., McElrath, M.J., Zolla-Pazner, S., Tomaras, G.D., Alam, S.M.,
1039 Evans, D.T., Montefiori, D.C., Karnasuta, C., Sutthent, R.*, et al.* (2012a). Immune-correlates
1040 analysis of an HIV-1 vaccine efficacy trial. N Engl J Med *366*, 1275-1286.
1041 Haynes, B.F., Kelsoe, G., Harrison, S.C., and Kepler, T.B. (2012b). B-cell-lineage immunogen
1042 design in vaccine development with HIV-1 as a case study. Nat Biotechnol *30*, 423-433.

1043 Heigele, A., Kmiec, D., Regensburger, K., Langer, S., Peiffer, L., Sturzel, C.M., Sauter, D.,
1044 Peeters, M., Pizzato, M., Learn, G.H., *et al.* (2016). The Potency of Nef-Mediated SERINC5
1045 Antagonism Correlates with the Prevalence of Primate Lentiviruses in the Wild. Cell Host
1046 Microbe *20*, 381-391.
1047 Herndler-Brandstetter, D., Shan, L., Yao, Y., Stecher, C., Plajer, V., Lietzenmayer, M., Strowig,
1048 T., de Zoete, M.R., Palm, N.W., Chen, J., *et al.* (2017). Humanized mouse model supports
1049 development, function, and tissue residency of human natural killer cells. Proc Natl Acad Sci U
1050 S A *114*, E9626-E9634.
1051 Hessell, A.J., Jaworski, J.P., Epson, E., Matsuda, K., Pandey, S., Kahl, C., Reed, J., Sutton, W.F.,
1052 Hammond, K.B., Cheever, T.A., *et al.* (2016). Early short-term treatment with neutralizing
1053 human monoclonal antibodies halts SHIV infection in infant macaques. Nat Med *22*, 362-368.
1054 Hessell, A.J., Shapiro, M.B., Powell, R., Malherbe, D.C., McBurney, S.P., Pandey, S., Cheever,
1055 T., Sutton, W.F., Kahl, C., Park, B., *et al.* (2018). Reduced Cell-Associated DNA and Improved
1056 Viral Control in Macaques following Passive Transfer of a Single Anti-V2 Monoclonal Antibody
1057 and Repeated Simian/Human Immunodeficiency Virus Challenges. J Virol *92*.
1058 Hioe, C.E., Li, G., Liu, X., Tsahouridis, O., He, X., Funaki, M., Klingler, J., Tang, A.F.,
1059 Feyznezhad, R., Heindel, D.W., *et al.* (2022). Non-neutralizing antibodies targeting the
1060 immunogenic regions of HIV-1 envelope reduce mucosal infection and virus burden in
1061 humanized mice. PLoS Pathog *18*, e1010183.
1062 Horton, H.M., Bernett, M.J., Peipp, M., Pong, E., Karki, S., Chu, S.Y., Richards, J.O., Chen, H.,
1063 Repp, R., Desjarlais, J.R., and Zhukovsky, E.A. (2010). Fc-engineered anti-CD40 antibody
1064 enhances multiple effector functions and exhibits potent in vitro and in vivo antitumor activity
1065 against hematologic malignancies. Blood *116*, 3004-3012.
1066 Horwitz, J.A., Bar-On, Y., Lu, C.L., Fera, D., Lockhart, A.A.K., Lorenzi, J.C.C., Nogueira, L.,
1067 Golijanin, J., Scheid, J.F., Seaman, M.S., *et al.* (2017). Non-neutralizing Antibodies Alter the
1068 Course of HIV-1 Infection In Vivo. Cell *170*, 637-648 e610.
1069 Horwitz, J.A., Halper-Stromberg, A., Mouquet, H., Gitlin, A.D., Tretiakova, A., Eisenreich,
1070 T.R., Malbec, M., Gravemann, S., Billerbeck, E., Dorner, M., *et al.* (2013). HIV-1 suppression
1071 and durable control by combining single broadly neutralizing antibodies and antiretroviral drugs
1072 in humanized mice. Proc Natl Acad Sci U S A *110*, 16538-16543.
1073 Hout, D.R., Gomez, M.L., Pacyniak, E., Gomez, L.M., Inbody, S.H., Mulcahy, E.R., Culley, N.,
1074 Pinson, D.M., Powers, M.F., Wong, S.W., and Stephens, E.B. (2005). Scrambling of the amino
1075 acids within the transmembrane domain of Vpu results in a simian-human immunodeficiency
1076 virus (SHIVTM) that is less pathogenic for pig-tailed macaques. Virology *339*, 56-69.
1077 Huang, C.C., Venturi, M., Majeed, S., Moore, M.J., Phogat, S., Zhang, M.Y., Dimitrov, D.S.,
1078 Hendrickson, W.A., Robinson, J., Sodroski, J., *et al.* (2004). Structural basis of tyrosine sulfation
1079 and VH-gene usage in antibodies that recognize the HIV type 1 coreceptor-binding site on
1080 gp120. Proc Natl Acad Sci U S A *101*, 2706-2711.
1081 Huang, J., Kang, B.H., Ishida, E., Zhou, T., Griesman, T., Sheng, Z., Wu, F., Doria-Rose, N.A.,
1082 Zhang, B., McKee, K., *et al.* (2016). Identification of a CD4-Binding-Site Antibody to HIV that
1083 Evolved Near-Pan Neutralization Breadth. Immunity *45*, 1108-1121.
1084 Huang, J., Kang, B.H., Pancera, M., Lee, J.H., Tong, T., Feng, Y., Imamichi, H., Georgiev, I.S.,
1085 Chuang, G.Y., Druz, A., *et al.* (2014). Broad and potent HIV-1 neutralization by a human
1086 antibody that binds the gp41-gp120 interface. Nature *515*, 138-142.

1087 Huang, J., Ofek, G., Laub, L., Louder, M.K., Doria-Rose, N.A., Longo, N.S., Imamichi, H.,
1088 Bailer, R.T., Chakrabarti, B., Sharma, S.K., *et al.* (2012). Broad and potent neutralization of
1089 HIV-1 by a gp41-specific human antibody. Nature *491*, 406-412.
1090 Jardine, J.G., Kulp, D.W., Havenar-Daughton, C., Sarkar, A., Briney, B., Sok, D., Sesterhenn, F.,
1091 Ereno-Orbea, J., Kalyuzhniy, O., Deresa, I., *et al.* (2016). HIV-1 broadly neutralizing antibody
1092 precursor B cells revealed by germline-targeting immunogen. Science *351*, 1458-1463.
1093 Jette, C.A., Barnes, C.O., Kirk, S.M., Melillo, B., Smith, A.B., 3rd, and Bjorkman, P.J. (2021).
1094 Cryo-EM structures of HIV-1 trimer bound to CD4-mimetics BNM-III-170 and M48U1 adopt a
1095 CD4-bound open conformation. Nat Commun *12*, 1950.
1096 Klein, F., Halper-Stromberg, A., Horwitz, J.A., Gruell, H., Scheid, J.F., Bournazos, S., Mouquet,
1097 H., Spatz, L.A., Diskin, R., Abadir, A., *et al.* (2012). HIV therapy by a combination of broadly
1098 neutralizing antibodies in humanized mice. Nature *492*, 118-122.
1099 Klein, F., Nogueira, L., Nishimura, Y., Phad, G., West, A.P., Jr., Halper-Stromberg, A., Horwitz,
1100 J.A., Gazumyan, A., Liu, C., Eisenreich, T.R., *et al.* (2014). Enhanced HIV-1 immunotherapy by
1101 commonly arising antibodies that target virus escape variants. J Exp Med *211*, 2361-2372.
1102 Kmiec, D., Iyer, S.S., Sturzel, C.M., Sauter, D., Hahn, B.H., and Kirchhoff, F. (2016). Vpu-
1103 Mediated Counteraction of Tetherin Is a Major Determinant of HIV-1 Interferon Resistance.
1104 MBio *7*.
1105 Kong, R., Xu, K., Zhou, T., Acharya, P., Lemmin, T., Liu, K., Ozorowski, G., Soto, C., Taft,
1106 J.D., Bailer, R.T., *et al.* (2016). Fusion peptide of HIV-1 as a site of vulnerability to neutralizing
1107 antibody. Science *352*, 828-833.
1108 Koyanagi, Y., Miles, S., Mitsuyasu, R.T., Merrill, J.E., Vinters, H.V., and Chen, I.S. (1987).
1109 Dual infection of the central nervous system by AIDS viruses with distinct cellular tropisms.
1110 Science *236*, 819-822.
1111 Krapp, C., Hotter, D., Gawanbacht, A., McLaren, P.J., Kluge, S.F., Sturzel, C.M., Mack, K.,
1112 Reith, E., Engelhart, S., Ciuffi, A., *et al.* (2016). Guanylate Binding Protein (GBP) 5 Is an
1113 Interferon-Inducible Inhibitor of HIV-1 Infectivity. Cell Host Microbe *19*, 504-514.
1114 Kwong, P.D., Wyatt, R., Robinson, J., Sweet, R.W., Sodroski, J., and Hendrickson, W.A. (1998).
1115 Structure of an HIV gp120 envelope glycoprotein in complex with the CD4 receptor and a
1116 neutralizing human antibody. Nature *393*, 648-659.
1117 Landais, E., and Moore, P.L. (2018). Development of broadly neutralizing antibodies in HIV-1
1118 infected elite neutralizers. Retrovirology *15*, 61.
1119 Langer, S.M., Hopfensperger, K., Iyer, S.S., Kreider, E.F., Learn, G.H., Lee, L.H., Hahn, B.H.,
1120 and Sauter, D. (2015). A Naturally Occurring rev1-vpu Fusion Gene Does Not Confer a Fitness
1121 Advantage to HIV-1. PLoS One *10*, e0142118.
1122 Laumaea, A., Smith, A.B., 3rd, Sodroski, J., and Finzi, A. (2020). Opening the HIV envelope:
1123 potential of CD4 mimics as multifunctional HIV entry inhibitors. Curr Opin HIV AIDS *15*, 300-
1124 308.
1125 Lee, J.H., Ozorowski, G., and Ward, A.B. (2016). Cryo-EM structure of a native, fully
1126 glycosylated, cleaved HIV-1 envelope trimer. Science *351*, 1043-1048.
1127 Lee, W.S., Richard, J., Lichtfuss, M., Smith, A.B., III, Park, J., Courter, J.R., Melillo, B.N.,
1128 Sodroski, J.G., Kaufmann, D.E., Finzi, A., *et al.* (2015). Antibody-Dependent Cellular
1129 Cytotoxicity against Reactivated HIV-1-Infected Cells. J Virol *90*, 2021-2030.
1130 Levesque, K., Zhao, Y.S., and Cohen, E.A. (2003). Vpu exerts a positive effect on HIV-1
1131 infectivity by down-modulating CD4 receptor molecules at the surface of HIV-1-producing cells.
1132 J Biol Chem *278*, 28346-28353.

Li, W., Chen, Y., Prevost, J., Ullah, I., Lu, M., Gong, S.Y., Tauzin, A., Gasser, R., Vezina, D., Anand, S.P., *et al.* (2021). Structural basis and mode of action for two broadly neutralizing antibodies against SARS-CoV-2 emerging variants of concern. Cell Rep, 110210.

Li, Y., Kappes, J.C., Conway, J.A., Price, R.W., Shaw, G.M., and Hahn, B.H. (1991). Molecular characterization of human immunodeficiency virus type 1 cloned directly from uncultured human brain tissue: identification of replication-competent and -defective viral genomes. J Virol *65*, 3973-3985.

Li, Z., Li, W., Lu, M., Bess, J., Jr., Chao, C.W., Gorman, J., Terry, D.S., Zhang, B., Zhou, T., Blanchard, S.C., *et al.* (2020). Subnanometer structures of HIV-1 envelope trimers on aldrithiol-2-inactivated virus particles. Nat Struct Mol Biol *27*, 726-734.

Liao, H.X., Lynch, R., Zhou, T., Gao, F., Alam, S.M., Boyd, S.D., Fire, A.Z., Roskin, K.M., Schramm, C.A., Zhang, Z., *et al.* (2013). Co-evolution of a broadly neutralizing HIV-1 antibody and founder virus. Nature *496*, 469-476.

Lu, C.L., Murakowski, D.K., Bournazos, S., Schoofs, T., Sarkar, D., Halper-Stromberg, A., Horwitz, J.A., Nogueira, L., Golijanin, J., Gazumyan, A., *et al.* (2016). Enhanced clearance of HIV-1-infected cells by broadly neutralizing antibodies against HIV-1 in vivo. Science *352*, 1001-1004.

Lu, M., Ma, X., Castillo-Menendez, L.R., Gorman, J., Alsahafi, N., Ermel, U., Terry, D.S., Chambers, M., Peng, D., Zhang, B., *et al.* (2019). Associating HIV-1 envelope glycoprotein structures with states on the virus observed by smFRET. Nature.

Lynch, R.M., Boritz, E., Coates, E.E., DeZure, A., Madden, P., Costner, P., Enama, M.E., Plummer, S., Holman, L., Hendel, C.S., *et al.* (2015). Virologic effects of broadly neutralizing antibody VRC01 administration during chronic HIV-1 infection. Science translational medicine *7*, 319ra206.

Madani, N., Princiotto, A.M., Easterhoff, D., Bradley, T., Luo, K., Williams, W.B., Liao, H.X., Moody, M.A., Phad, G.E., Vazquez Bernat, N., *et al.* (2016). Antibodies Elicited by Multiple Envelope Glycoprotein Immunogens in Primates Neutralize Primary Human Immunodeficiency Viruses (HIV-1) Sensitized by CD4-Mimetic Compounds. J Virol *90*, 5031-5046.

Madani, N., Princiotto, A.M., Mach, L., Ding, S., Prevost, J., Richard, J., Hora, B., Sutherland, L., Zhao, C.A., Conn, B.P., *et al.* (2018). A CD4-mimetic compound enhances vaccine efficacy against stringent immunodeficiency virus challenge. Nat Commun *9*, 2363.

Manganaro, L., Hong, P., Hernandez, M.M., Argyle, D., Mulder, L.C.F., Potla, U., Diaz-Griffero, F., Lee, B., Fernandez-Sesma, A., and Simon, V. (2018). IL-15 regulates susceptibility of CD4(+) T cells to HIV infection. Proc Natl Acad Sci U S A *115*, E9659-E9667.

Matusali, G., Potesta, M., Santoni, A., Cerboni, C., and Doria, M. (2012). The human immunodeficiency virus type 1 Nef and Vpu proteins downregulate the natural killer cell-activating ligand PVR. J Virol *86*, 4496-4504.

McCune, J.M., Rabin, L.B., Feinberg, M.B., Lieberman, M., Kosek, J.C., Reyes, G.R., and Weissman, I.L. (1988). Endoproteolytic cleavage of gp160 is required for the activation of human immunodeficiency virus. Cell *53*, 55-67.

Melillo, B., Liang, S., Park, J., Schon, A., Courter, J.R., LaLonde, J.M., Wendler, D.J., Princiotto, A.M., Seaman, M.S., Freire, E., *et al.* (2016). Small-Molecule CD4-Mimics: Structure-Based Optimization of HIV-1 Entry Inhibition. ACS Med Chem Lett *7*, 330-334.

Moog, C., Dereuddre-Bosquet, N., Teillaud, J.L., Biedma, M.E., Holl, V., Van Ham, G., Heyndrickx, L., Van Dorsselaer, A., Katinger, D., Vcelar, B., *et al.* (2014). Protective effect of

1178 vaginal application of neutralizing and nonneutralizing inhibitory antibodies against vaginal
1179 SHIV challenge in macaques. Mucosal Immunol *7*, 46-56.
1180 Mouquet, H., Scharf, L., Euler, Z., Liu, Y., Eden, C., Scheid, J.F., Halper-Stromberg, A.,
1181 Gnanapragasam, P.N., Spencer, D.I., Seaman, M.S.*, et al.* (2012). Complex-type N-glycan
1182 recognition by potent broadly neutralizing HIV antibodies. Proc Natl Acad Sci U S A *109*,
1183 E3268-3277.
1184 Munro, J.B., Gorman, J., Ma, X., Zhou, Z., Arthos, J., Burton, D.R., Koff, W.C., Courter, J.R.,
1185 Smith, A.B., III, Kwong, P.D.*, et al.* (2014). Conformational dynamics of single HIV-1 envelope
1186 trimers on the surface of native virions. Science *346*, 759-763.
1187 Neil, S.J., Eastman, S.W., Jouvenet, N., and Bieniasz, P.D. (2006). HIV-1 Vpu promotes release
1188 and prevents endocytosis of nascent retrovirus particles from the plasma membrane. PLoS
1189 Pathog *2*, e39.
1190 Neil, S.J., Zang, T., and Bieniasz, P.D. (2008). Tetherin inhibits retrovirus release and is
1191 antagonized by HIV-1 Vpu. Nature *451*, 425-430.
1192 Nishimura, Y., Gautam, R., Chun, T.W., Sadjadpour, R., Foulds, K.E., Shingai, M., Klein, F.,
1193 Gazumyan, A., Golijanin, J., Donaldson, M.*, et al.* (2017). Early antibody therapy can induce
1194 long-lasting immunity to SHIV. Nature *543*, 559-563.
1195 Ochsenbauer, C., Edmonds, T.G., Ding, H., Keele, B.F., Decker, J., Salazar, M.G., Salazar-
1196 Gonzalez, J.F., Shattock, R., Haynes, B.F., Shaw, G.M.*, et al.* (2012). Generation of
1197 Transmitted/Founder HIV-1 Infectious Molecular Clones and Characterization of Their
1198 Replication Capacity in CD4 T Lymphocytes and Monocyte-Derived Macrophages. J Virol *86*,
1199 2715-2728.
1200 Parrish, N.F., Gao, F., Li, H., Giorgi, E.E., Barbian, H.J., Parrish, E.H., Zajic, L., Iyer, S.S.,
1201 Decker, J.M., Kumar, A.*, et al.* (2013). Phenotypic properties of transmitted founder HIV-1. Proc
1202 Natl Acad Sci U S A *110*, 6626-6633.
1203 Parrish, N.F., Wilen, C.B., Banks, L.B., Iyer, S.S., Pfaff, J.M., Salazar-Gonzalez, J.F., Salazar,
1204 M.G., Decker, J.M., Parrish, E.H., Berg, A.*, et al.* (2012). Transmitted/founder and chronic
1205 subtype C HIV-1 use CD4 and CCR5 receptors with equal efficiency and are not inhibited by
1206 blocking the integrin alpha4beta7. PLoS Pathog *8*, e1002686.
1207 Parsons, M.S., Lee, W.S., Kristensen, A.B., Amarasena, T., Khoury, G., Wheatley, A.K.,
1208 Reynaldi, A., Wines, B.D., Hogarth, P.M., Davenport, M.P., and Kent, S.J. (2019). Fc-dependent
1209 functions are redundant to efficacy of anti-HIV antibody PGT121 in macaques. J Clin Invest
1210 *129*, 182-191.
1211 Pauthner, M.G., Nkolola, J.P., Havenar-Daughton, C., Murrell, B., Reiss, S.M., Bastidas, R.,
1212 Prevost, J., Nedellec, R., von Bredow, B., Abbink, P.*, et al.* (2019). Vaccine-Induced Protection
1213 from Homologous Tier 2 SHIV Challenge in Nonhuman Primates Depends on Serum-
1214 Neutralizing Antibody Titers. Immunity *50*, 241-252 e246.
1215 Phad, G.E., Vazquez Bernat, N., Feng, Y., Ingale, J., Martinez Murillo, P.A., O'Dell, S., Li, Y.,
1216 Mascola, J.R., Sundling, C., Wyatt, R.T., and Karlsson Hedestam, G.B. (2015). Diverse antibody
1217 genetic and recognition properties revealed following HIV-1 envelope glycoprotein
1218 immunization. J Immunol *194*, 5903-5914.
1219 Pham, T.N., Lukhele, S., Dallaire, F., Perron, G., and Cohen, E.A. (2016). Enhancing Virion
1220 Tethering by BST2 Sensitizes Productively and Latently HIV-infected T cells to ADCC
1221 Mediated by Broadly Neutralizing Antibodies. Sci Rep *6*, 37225.

Platt, E.J., Wehrly, K., Kuhmann, S.E., Chesebro, B., and Kabat, D. (1998). Effects of CCR5 and CD4 cell surface concentrations on infections by macrophagetropic isolates of human immunodeficiency virus type 1. J Virol *72*, 2855-2864.

Prevost, J., Edgar, C.R., Richard, J., Trothen, S.M., Jacob, R.A., Mumby, M.J., Pickering, S., Dube, M., Kaufmann, D.E., Kirchhoff, F.*, et al.* (2020a). HIV-1 Vpu Downregulates Tim-3 from the Surface of Infected CD4(+) T Cells. J Virol *94*.

Prevost, J., Medjahed, H., Vezina, D., Chen, H.C., Hahn, B.H., Smith, A.B., 3rd, and Finzi, A. (2021). HIV-1 Envelope Glycoproteins Proteolytic Cleavage Protects Infected Cells from ADCC Mediated by Plasma from Infected Individuals. Viruses *13*.

Prevost, J., Pickering, S., Mumby, M.J., Medjahed, H., Gendron-Lepage, G., Delgado, G.G., Dirk, B.S., Dikeakos, J.D., Sturzel, C.M., Sauter, D.*, et al.* (2019). Upregulation of BST-2 by Type I Interferons Reduces the Capacity of Vpu To Protect HIV-1-Infected Cells from NK Cell Responses. mBio *10*.

Prevost, J., Richard, J., Ding, S., Pacheco, B., Charlebois, R., Hahn, B.H., Kaufmann, D.E., and Finzi, A. (2018a). Envelope glycoproteins sampling states 2/3 are susceptible to ADCC by sera from HIV-1-infected individuals. Virology *515*, 38-45.

Prevost, J., Richard, J., Gasser, R., Medjahed, H., Kirchhoff, F., Hahn, B.H., Kappes, J.C., Ochsenbauer, C., Duerr, R., and Finzi, A. (2022). Detection of the HIV-1 accessory proteins Nef and Vpu by flow cytometry represents a new tool to study their functional interplay within a single infected CD4+ T cell. J Virol, jvi0192921.

Prevost, J., Richard, J., Medjahed, H., Alexander, A., Jones, J., Kappes, J.C., Ochsenbauer, C., and Finzi, A. (2018b). Incomplete Downregulation of CD4 Expression Affects HIV-1 Env Conformation and Antibody-Dependent Cellular Cytotoxicity Responses. J Virol *92*.

Prevost, J., Tolbert, W.D., Medjahed, H., Sherburn, R.T., Madani, N., Zoubchenok, D., Gendron-Lepage, G., Gaffney, A.E., Grenier, M.C., Kirk, S.*, et al.* (2020b). The HIV-1 Env gp120 Inner Domain Shapes the Phe43 Cavity and the CD4 Binding Site. mBio *11*.

Prevost, J., Zoubchenok, D., Richard, J., Veillette, M., Pacheco, B., Coutu, M., Brassard, N., Parsons, M.S., Ruxrungtham, K., Bunupuradah, T.*, et al.* (2017). Influence of the Envelope gp120 Phe 43 Cavity on HIV-1 Sensitivity to Antibody-Dependent Cell-Mediated Cytotoxicity Responses. J Virol *91*.

Rajashekar, J.K., Richard, J., Beloor, J., Prevost, J., Anand, S.P., Beaudoin-Bussieres, G., Shan, L., Herndler-Brandstetter, D., Gendron-Lepage, G., Medjahed, H.*, et al.* (2021). Modulating HIV-1 envelope glycoprotein conformation to decrease the HIV-1 reservoir. Cell Host Microbe *29*, 904-916 e906.

Rerks-Ngarm, S., Pitisuttithum, P., Nitayaphan, S., Kaewkungwal, J., Chiu, J., Paris, R., Premsri, N., Namwat, C., de Souza, M., Adams, E.*, et al.* (2009). Vaccination with ALVAC and AIDSVAX to prevent HIV-1 infection in Thailand. N Engl J Med *361*, 2209-2220.

Richard, J., Pacheco, B., Gohain, N., Veillette, M., Ding, S., Alsahafi, N., Tolbert, W.D., Prevost, J., Chapleau, J.P., Coutu, M.*, et al.* (2016). Co-receptor Binding Site Antibodies Enable CD4-Mimetics to Expose Conserved Anti-cluster A ADCC Epitopes on HIV-1 Envelope Glycoproteins. EBioMedicine *12*, 208-218.

Richard, J., Prevost, J., von Bredow, B., Ding, S., Brassard, N., Medjahed, H., Coutu, M., Melillo, B., Bibollet-Ruche, F., Hahn, B.H.*, et al.* (2017). BST-2 Expression Modulates Small CD4-Mimetic Sensitization of HIV-1-Infected Cells to Antibody-Dependent Cellular Cytotoxicity. J Virol *91*.

1267 Richard, J., Veillette, M., Brassard, N., Iyer, S.S., Roger, M., Martin, L., Pazgier, M., Schon, A.,
1268 Freire, E., Routy, J.P., *et al.* (2015). CD4 mimetics sensitize HIV-1-infected cells to ADCC. Proc
1269 Natl Acad Sci U S A *112*, E2687-2694.
1270 Robinson, C.A., Lyddon, T.D., Gil, H.M., Evans, D.T., Kuzmichev, Y.V., Richard, J., Finzi, A.,
1271 Welbourn, S., Rasmussen, L., Miranda Nebane, N., *et al.* (2021). Novel compound inhibitors of
1272 HIV-1 NL4-3 Vpu. bioRxiv.
1273 Robinson JE, Y.H., Holton D, Elliott S, Ho DD (1992). Distinct antigenic sites on HIV gp120
1274 identified by a panel of human monoclonal antibodies. Journal of Cellular Biochemistry
1275 Supplement *16E*, Q449.
1276 Rudicell, R.S., Kwon, Y.D., Ko, S.Y., Pegu, A., Louder, M.K., Georgiev, I.S., Wu, X., Zhu, J.,
1277 Boyington, J.C., Chen, X., *et al.* (2014). Enhanced Potency of a Broadly Neutralizing HIV-1
1278 Antibody In Vitro Improves Protection against Lentiviral Infection In Vivo. J Virol *88*, 12669-
1279 12682.
1280 Sajadi, M.M., Dashti, A., Rikhtegaran Tehrani, Z., Tolbert, W.D., Seaman, M.S., Ouyang, X.,
1281 Gohain, N., Pazgier, M., Kim, D., Cavet, G., *et al.* (2018). Identification of Near-Pan-
1282 neutralizing Antibodies against HIV-1 by Deconvolution of Plasma Humoral Responses. Cell
1283 *173*, 1783-1795 e1714.
1284 Salazar-Gonzalez, J.F., Salazar, M.G., Keele, B.F., Learn, G.H., Giorgi, E.E., Li, H., Decker,
1285 J.M., Wang, S., Baalwa, J., Kraus, M.H., *et al.* (2009). Genetic identity, biological phenotype,
1286 and evolutionary pathways of transmitted/founder viruses in acute and early HIV-1 infection. J
1287 Exp Med *206*, 1273-1289.
1288 Santra, S., Tomaras, G.D., Warrier, R., Nicely, N.I., Liao, H.X., Pollara, J., Liu, P., Alam, S.M.,
1289 Zhang, R., Cocklin, S.L., *et al.* (2015). Human Non-neutralizing HIV-1 Envelope Monoclonal
1290 Antibodies Limit the Number of Founder Viruses during SHIV Mucosal Infection in Rhesus
1291 Macaques. PLoS Pathog *11*, e1005042.
1292 Sato, K., Misawa, N., Fukuhara, M., Iwami, S., An, D.S., Ito, M., and Koyanagi, Y. (2012). Vpu
1293 augments the initial burst phase of HIV-1 propagation and downregulates BST2 and CD4 in
1294 humanized mice. J Virol *86*, 5000-5013.
1295 Saunders, K.O., Wiehe, K., Tian, M., Acharya, P., Bradley, T., Alam, S.M., Go, E.P., Scearce,
1296 R., Sutherland, L., Henderson, R., *et al.* (2019). Targeted selection of HIV-specific antibody
1297 mutations by engineering B cell maturation. Science *366*.
1298 Sauter, D., Hotter, D., Van Driessche, B., Sturzel, C.M., Kluge, S.F., Wildum, S., Yu, H.,
1299 Baumann, B., Wirth, T., Plantier, J.C., *et al.* (2015). Differential regulation of NF-kappaB-
1300 mediated proviral and antiviral host gene expression by primate lentiviral Nef and Vpu proteins.
1301 Cell Rep *10*, 586-599.
1302 Scheid, J.F., Horwitz, J.A., Bar-On, Y., Kreider, E.F., Lu, C.L., Lorenzi, J.C., Feldmann, A.,
1303 Braunschweig, M., Nogueira, L., Oliveira, T., *et al.* (2016). HIV-1 antibody 3BNC117
1304 suppresses viral rebound in humans during treatment interruption. Nature *535*, 556-560.
1305 Scheid, J.F., Mouquet, H., Ueberheide, B., Diskin, R., Klein, F., Oliveira, T.Y., Pietzsch, J.,
1306 Fenyo, D., Abadir, A., Velinzon, K., *et al.* (2011). Sequence and structural convergence of broad
1307 and potent HIV antibodies that mimic CD4 binding. Science *333*, 1633-1637.
1308 Schommers, P., Gruell, H., Abernathy, M.E., Tran, M.K., Dingens, A.S., Gristick, H.B., Barnes,
1309 C.O., Schoofs, T., Schlotz, M., Vanshylla, K., *et al.* (2020). Restriction of HIV-1 Escape by a
1310 Highly Broad and Potent Neutralizing Antibody. Cell *180*, 471-489 e422.

1311 Schoofs, T., Barnes, C.O., Suh-Toma, N., Golijanin, J., Schommers, P., Gruell, H., West, A.P.,
1312 Jr., Bach, F., Lee, Y.E., Nogueira, L.*, et al.* (2019). Broad and Potent Neutralizing Antibodies
1313 Recognize the Silent Face of the HIV Envelope. Immunity *50*, 1513-1529 e1519.
1314 Shah, A.H., Sowrirajan, B., Davis, Z.B., Ward, J.P., Campbell, E.M., Planelles, V., and Barker,
1315 E. (2010). Degranulation of natural killer cells following interaction with HIV-1-infected cells is
1316 hindered by downmodulation of NTB-A by Vpu. Cell Host Microbe *8*, 397-409.
1317 Shaik, M.M., Peng, H., Lu, J., Rits-Volloch, S., Xu, C., Liao, M., and Chen, B. (2019). Structural
1318 basis of coreceptor recognition by HIV-1 envelope spike. Nature *565*, 318-323.
1319 Shaw, G.M., Hahn, B.H., Arya, S.K., Groopman, J.E., Gallo, R.C., and Wong-Staal, F. (1984).
1320 Molecular characterization of human T-cell leukemia (lymphotropic) virus type III in the
1321 acquired immune deficiency syndrome. Science *226*, 1165-1171.
1322 Shingai, M., Nishimura, Y., Klein, F., Mouquet, H., Donau, O.K., Plishka, R., Buckler-White,
1323 A., Seaman, M., Piatak, M., Jr., Lifson, J.D.*, et al.* (2013). Antibody-mediated immunotherapy of
1324 macaques chronically infected with SHIV suppresses viraemia. Nature *503*, 277-280.
1325 Shingai, M., Yoshida, T., Martin, M.A., and Strebel, K. (2011). Some human immunodeficiency
1326 virus type 1 Vpu proteins are able to antagonize macaque BST-2 in vitro and in vivo: Vpu-
1327 negative simian-human immunodeficiency viruses are attenuated in vivo. J Virol *85*, 9708-9715.
1328 Smith, P., DiLillo, D.J., Bournazos, S., Li, F., and Ravetch, J.V. (2012). Mouse model
1329 recapitulating human Fcgamma receptor structural and functional diversity. Proc Natl Acad Sci
1330 U S A *109*, 6181-6186.
1331 Sojar, H., Baron, S., Sullivan, J.T., Garrett, M., van Haaren, M.M., Hoffman, J., Overbaugh, J.,
1332 Doranz, B.J., and Hicar, M.D. (2019). Monoclonal Antibody 2C6 Targets a Cross-Clade
1333 Conformational Epitope in gp41 with Highly Active Antibody-Dependent Cell Cytotoxicity. J
1334 Virol *93*.
1335 Sok, D., Le, K.M., Vadnais, M., Saye-Francisco, K.L., Jardine, J.G., Torres, J.L., Berndsen, Z.T.,
1336 Kong, L., Stanfield, R., Ruiz, J.*, et al.* (2017). Rapid elicitation of broadly neutralizing antibodies
1337 to HIV by immunization in cows. Nature *548*, 108-111.
1338 Stadtmueller, B.M., Bridges, M.D., Dam, K.M., Lerch, M.T., Huey-Tubman, K.E., Hubbell,
1339 W.L., and Bjorkman, P.J. (2018). DEER Spectroscopy Measurements Reveal Multiple
1340 Conformations of HIV-1 SOSIP Envelopes that Show Similarities with Envelopes on Native
1341 Virions. Immunity *49*, 235-246 e234.
1342 Steichen, J.M., Kulp, D.W., Tokatlian, T., Escolano, A., Dosenovic, P., Stanfield, R.L., McCoy,
1343 L.E., Ozorowski, G., Hu, X., Kalyuzhniy, O.*, et al.* (2016). HIV Vaccine Design to Target
1344 Germline Precursors of Glycan-Dependent Broadly Neutralizing Antibodies. Immunity *45*, 483-
1345 496.
1346 Stiegler, G., Kunert, R., Purtscher, M., Wolbank, S., Voglauer, R., Steindl, F., and Katinger, H.
1347 (2001). A potent cross-clade neutralizing human monoclonal antibody against a novel epitope on
1348 gp41 of human immunodeficiency virus type 1. AIDS Res Hum Retroviruses *17*, 1757-1765.
1349 Theodore, T.S., Englund, G., Buckler-White, A., Buckler, C.E., Martin, M.A., and Peden, K.W.
1350 (1996). Construction and characterization of a stable full-length macrophage-tropic HIV type 1
1351 molecular clone that directs the production of high titers of progeny virions. AIDS Res Hum
1352 Retroviruses *12*, 191-194.
1353 Tolbert, W.D., Sherburn, R., Gohain, N., Ding, S., Flinko, R., Orlandi, C., Ray, K., Finzi, A.,
1354 Lewis, G.K., and Pazgier, M. (2020). Defining rules governing recognition and Fc-mediated
1355 effector functions to the HIV-1 co-receptor binding site. BMC Biol *18*, 91.

1356 Tomaras, G.D., and Haynes, B.F. (2009). HIV-1-specific antibody responses during acute and
1357 chronic HIV-1 infection. Curr Opin HIV AIDS *4*, 373-379.
1358 Tomaras, G.D., Yates, N.L., Liu, P., Qin, L., Fouda, G.G., Chavez, L.L., Decamp, A.C., Parks,
1359 R.J., Ashley, V.C., Lucas, J.T.*, et al.* (2008). Initial B-cell responses to transmitted human
1360 immunodeficiency virus type 1: virion-binding immunoglobulin M (IgM) and IgG antibodies
1361 followed by plasma anti-gp41 antibodies with ineffective control of initial viremia. J Virol *82*,
1362 12449-12463.
1363 Van Damme, N., Goff, D., Katsura, C., Jorgenson, R.L., Mitchell, R., Johnson, M.C., Stephens,
1364 E.B., and Guatelli, J. (2008). The interferon-induced protein BST-2 restricts HIV-1 release and is
1365 downregulated from the cell surface by the viral Vpu protein. Cell Host Microbe *3*, 245-252.
1366 Vanshylla, K., Held, K., Eser, T.M., Gruell, H., Kleipass, F., Stumpf, R., Jain, K., Weiland, D.,
1367 Munch, J., Gruttner, B.*, et al.* (2021). CD34T+ Humanized Mouse Model to Study Mucosal
1368 HIV-1 Transmission and Prevention. Vaccines (Basel) *9*.
1369 Veillette, M., Coutu, M., Richard, J., Batraville, L.A., Dagher, O., Bernard, N., Tremblay, C.,
1370 Kaufmann, D.E., Roger, M., and Finzi, A. (2015). The HIV-1 gp120 CD4-Bound Conformation
1371 Is Preferentially Targeted by Antibody-Dependent Cellular Cytotoxicity-Mediating Antibodies in
1372 Sera from HIV-1-Infected Individuals. J Virol *89*, 545-551.
1373 Veillette, M., Desormeaux, A., Medjahed, H., Gharsallah, N.E., Coutu, M., Baalwa, J., Guan, Y.,
1374 Lewis, G., Ferrari, G., Hahn, B.H.*, et al.* (2014). Interaction with cellular CD4 exposes HIV-1
1375 envelope epitopes targeted by antibody-dependent cell-mediated cytotoxicity. J Virol *88*, 2633-
1376 2644.
1377 Visciano, M.L., Gohain, N., Sherburn, R., Orlandi, C., Flinko, R., Dashti, A., Lewis, G.K.,
1378 Tolbert, W.D., and Pazgier, M. (2019). Induction of Fc-Mediated Effector Functions Against a
1379 Stabilized Inner Domain of HIV-1 gp120 Designed to Selectively Harbor the A32 Epitope
1380 Region. Front Immunol *10*, 677.
1381 von Bredow, B., Arias, J.F., Heyer, L.N., Moldt, B., Le, K., Robinson, J.E., Zolla-Pazner, S.,
1382 Burton, D.R., and Evans, D.T. (2016). Comparison of Antibody-Dependent Cell-Mediated
1383 Cytotoxicity and Virus Neutralization by HIV-1 Env-Specific Monoclonal Antibodies. J Virol
1384 *90*, 6127-6139.
1385 Walker, L.M., Huber, M., Doores, K.J., Falkowska, E., Pejchal, R., Julien, J.P., Wang, S.K.,
1386 Ramos, A., Chan-Hui, P.Y., Moyle, M.*, et al.* (2011). Broad neutralization coverage of HIV by
1387 multiple highly potent antibodies. Nature *477*, 466-470.
1388 Walker, L.M., Phogat, S.K., Chan-Hui, P.Y., Wagner, D., Phung, P., Goss, J.L., Wrin, T., Simek,
1389 M.D., Fling, S., Mitcham, J.L.*, et al.* (2009). Broad and potent neutralizing antibodies from an
1390 African donor reveal a new HIV-1 vaccine target. Science *326*, 285-289.
1391 Wang, P., Gajjar, M.R., Yu, J., Padte, N.N., Gettie, A., Blanchard, J.L., Russell-Lodrigue, K.,
1392 Liao, L.E., Perelson, A.S., Huang, Y., and Ho, D.D. (2020). Quantifying the contribution of Fc-
1393 mediated effector functions to the antiviral activity of anti-HIV-1 IgG1 antibodies in vivo. Proc
1394 Natl Acad Sci U S A *117*, 18002-18009.
1395 Weissenhorn, W., Dessen, A., Harrison, S.C., Skehel, J.J., and Wiley, D.C. (1997). Atomic
1396 structure of the ectodomain from HIV-1 gp41. Nature *387*, 426-430.
1397 Williams, K.L., Stumpf, M., Naiman, N.E., Ding, S., Garrett, M., Gobillot, T., Vezina, D.,
1398 Dusenbury, K., Ramadoss, N.S., Basom, R.*, et al.* (2019). Identification of HIV gp41-specific
1399 antibodies that mediate killing of infected cells. PLoS Pathog *15*, e1007572.

Williams, W.B., Zhang, J., Jiang, C., Nicely, N.I., Fera, D., Luo, K., Moody, M.A., Liao, H.X., Alam, S.M., Kepler, T.B.*, et al.* (2017). Initiation of HIV neutralizing B cell lineages with sequential envelope immunizations. Nat Commun *8*, 1732.

Wines, B.D., Billings, H., McLean, M.R., Kent, S.J., and Hogarth, P.M. (2017). Antibody Functional Assays as Measures of Fc Receptor-Mediated Immunity to HIV - New Technologies and their Impact on the HIV Vaccine Field. Curr HIV Res *15*, 202-215.

Wines, B.D., Vanderven, H.A., Esparon, S.E., Kristensen, A.B., Kent, S.J., and Hogarth, P.M. (2016). Dimeric FcgammaR Ectodomains as Probes of the Fc Receptor Function of Anti-Influenza Virus IgG. J Immunol *197*, 1507-1516.

Wu, B., Chien, E.Y., Mol, C.D., Fenalti, G., Liu, W., Katritch, V., Abagyan, R., Brooun, A., Wells, P., Bi, F.C.*, et al.* (2010a). Structures of the CXCR4 chemokine GPCR with small-molecule and cyclic peptide antagonists. Science *330*, 1066-1071.

Wu, X., Yang, Z.Y., Li, Y., Hogerkorp, C.M., Schief, W.R., Seaman, M.S., Zhou, T., Schmidt, S.D., Wu, L., Xu, L.*, et al.* (2010b). Rational design of envelope identifies broadly neutralizing human monoclonal antibodies to HIV-1. Science *329*, 856-861.

Xu, J.Y., Gorny, M.K., Palker, T., Karwowska, S., and Zolla-Pazner, S. (1991). Epitope mapping of two immunodominant domains of gp41, the transmembrane protein of human immunodeficiency virus type 1, using ten human monoclonal antibodies. J Virol *65*, 4832-4838.

Yamada, E., Nakaoka, S., Klein, L., Reith, E., Langer, S., Hopfensperger, K., Iwami, S., Schreiber, G., Kirchhoff, F., Koyanagi, Y.*, et al.* (2018). Human-Specific Adaptations in Vpu Conferring Anti-tetherin Activity Are Critical for Efficient Early HIV-1 Replication In Vivo. Cell Host Microbe *23*, 110-120 e117.

Yang, Z., Liu, X., Sun, Z., Li, J., Tan, W., Yu, W., and Zhang, M. (2018). Identification of a HIV Gp41-Specific Human Monoclonal Antibody With Potent Antibody-Dependent Cellular Cytotoxicity. Front Immunol *9*, 2613.

Yang, Z., Wang, H., Liu, A.Z., Gristick, H.B., and Bjorkman, P.J. (2019). Asymmetric opening of HIV-1 Env bound to CD4 and a coreceptor-mimicking antibody. Nat Struct Mol Biol *26*, 1167-1175.

Zhou, T., Lynch, R.M., Chen, L., Acharya, P., Wu, X., Doria-Rose, N.A., Joyce, M.G., Lingwood, D., Soto, C., Bailer, R.T.*, et al.* (2015). Structural Repertoire of HIV-1-Neutralizing Antibodies Targeting the CD4 Supersite in 14 Donors. Cell *161*, 1280-1292.

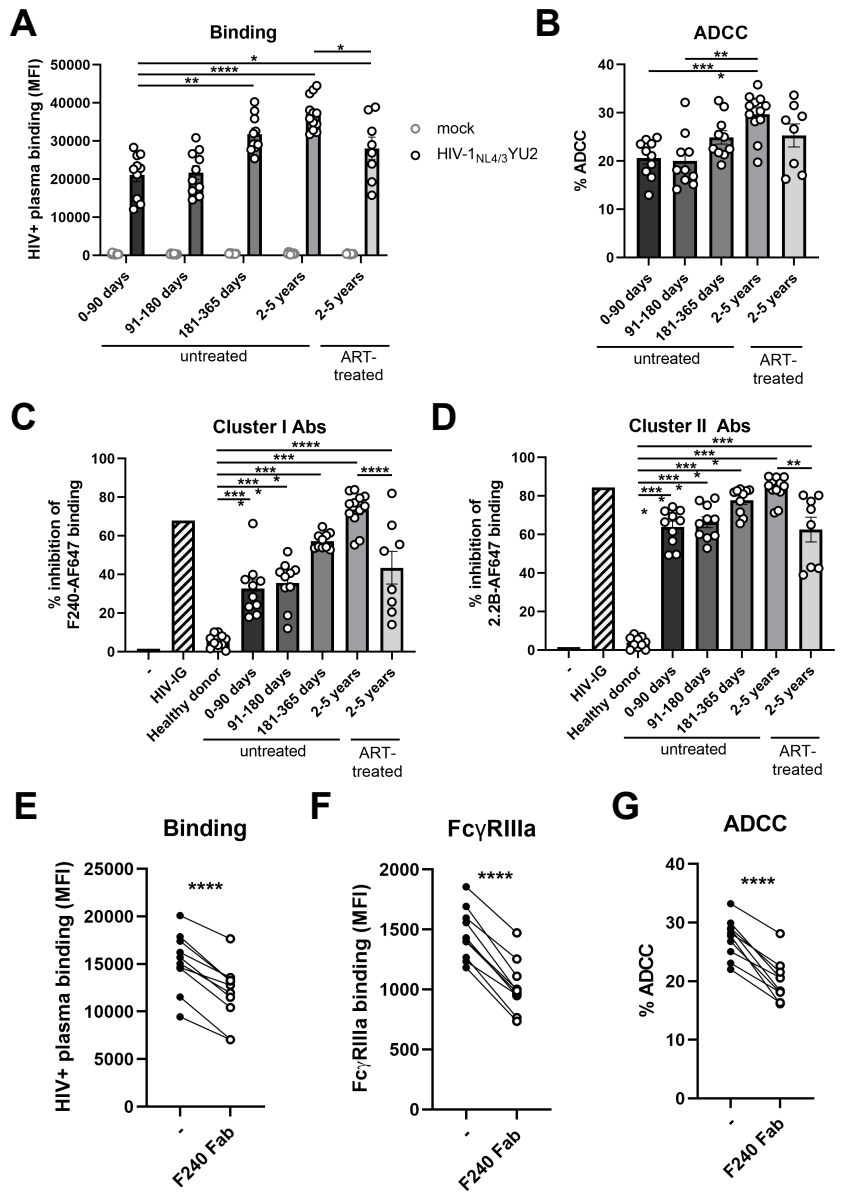
A
Binding
HIV+ plasma binding (MFI)
50000
40000
30000
20000
10000
0
mock
HIV-1NL4/3YU2
0-90 days
91-180 days
181-365 days
2-5 years
2-5 years
untreated
ART-treated
B
ADCC
% ADCC
40
30
20
10
0
C
Cluster I Abs
% inhibition of F240-AF647 binding
100
80
60
40
20
0
-
HIV-IG
Healthy donor
D
Cluster II Abs
% inhibition of 2.2B-AF647 binding
E
Binding
HIV+ plasma binding (MFI)
25000
20000
15000
10000
5000
F240 Fab
F
FcγRIIIa
FcγRIIIa binding (MFI)
2000
1500
1000
500
G
ADCC
% ADCC

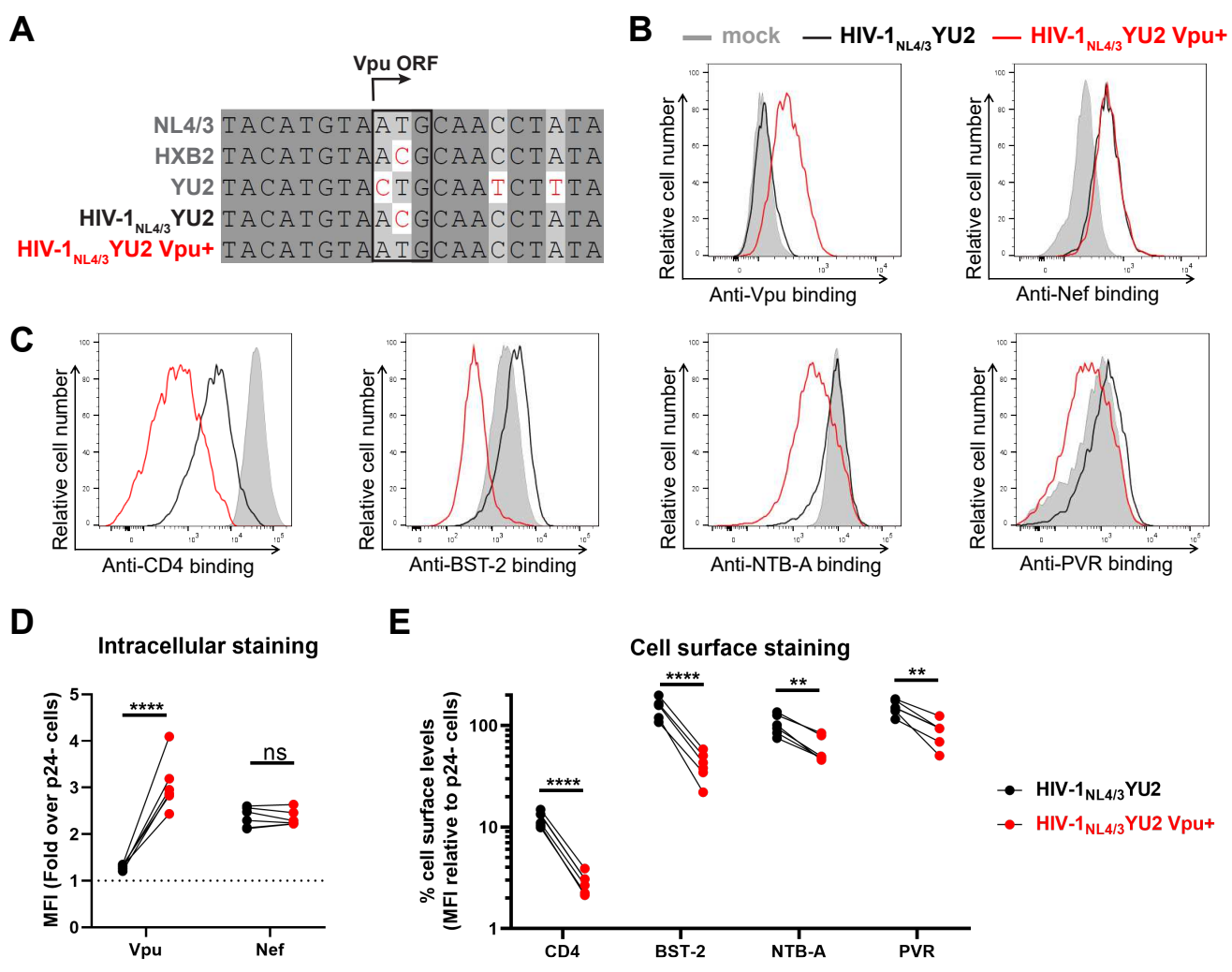
A
Vpu ORF
NL4/3 TACATGTAATGCAACCTATA
HXB2 TACATGTAACGCAACCTATA
YU2 TACATGTACTGCAATCTTTA
HIV-1NL4/3YU2 TACATGTAACGCAACCTATA
HIV-1NL4/3YU2 Vpu+ TACATGTAATGCAACCTATA
B
mock
HIV-1NL4/3YU2
HIV-1NL4/3YU2 Vpu+
Relative cell number
Anti-Vpu binding
Anti-Nef binding
C
Anti-CD4 binding
Anti-BST-2 binding
Anti-NTB-A binding
Anti-PVR binding
D
Intracellular staining
MFI (Fold over p24- cells)
****
ns
Vpu
Nef
E
Cell surface staining
% cell surface levels (MFI relative to p24- cells)
****
****
**
**
CD4
BST-2
NTB-A
PVR
HIV-1NL4/3YU2
HIV-1NL4/3YU2 Vpu+

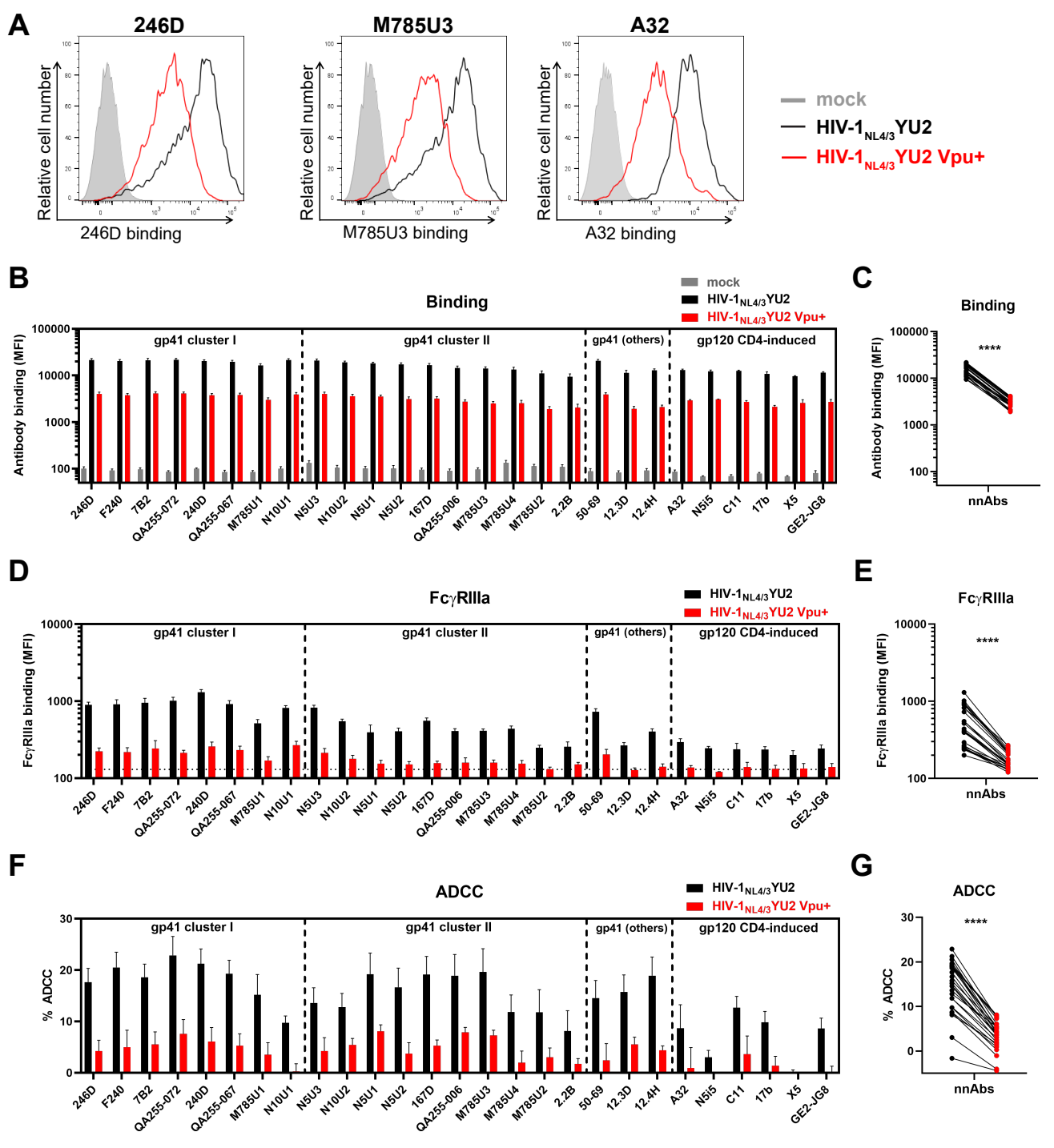
A
246D
M785U3
A32
Relative cell number
246D binding
M785U3 binding
A32 binding
mock
HIV-1NL4/3YU2
HIV-1NL4/3YU2 Vpu+
B
Binding
Antibody binding (MFI)
gp41 cluster I
gp41 cluster II
gp41 (others)
gp120 CD4-induced
246D F240 7B2 QA255-072 240D QA255-067 M785U1 N10U1 N5U3 N10U2 N5U1 N5U2 167D QA255-006 M785U3 M785U4 M785U2 2.2B 50-69 12.3D 12.4H A32 N5i5 C11 17b X5 GE2-JG8
C
Binding
****
nnAbs
D
FcγRIIIa
FcγRIIIa binding (MFI)
E
FcγRIIIa
****
nnAbs
F
ADCC
% ADCC
G
ADCC
****
nnAbs

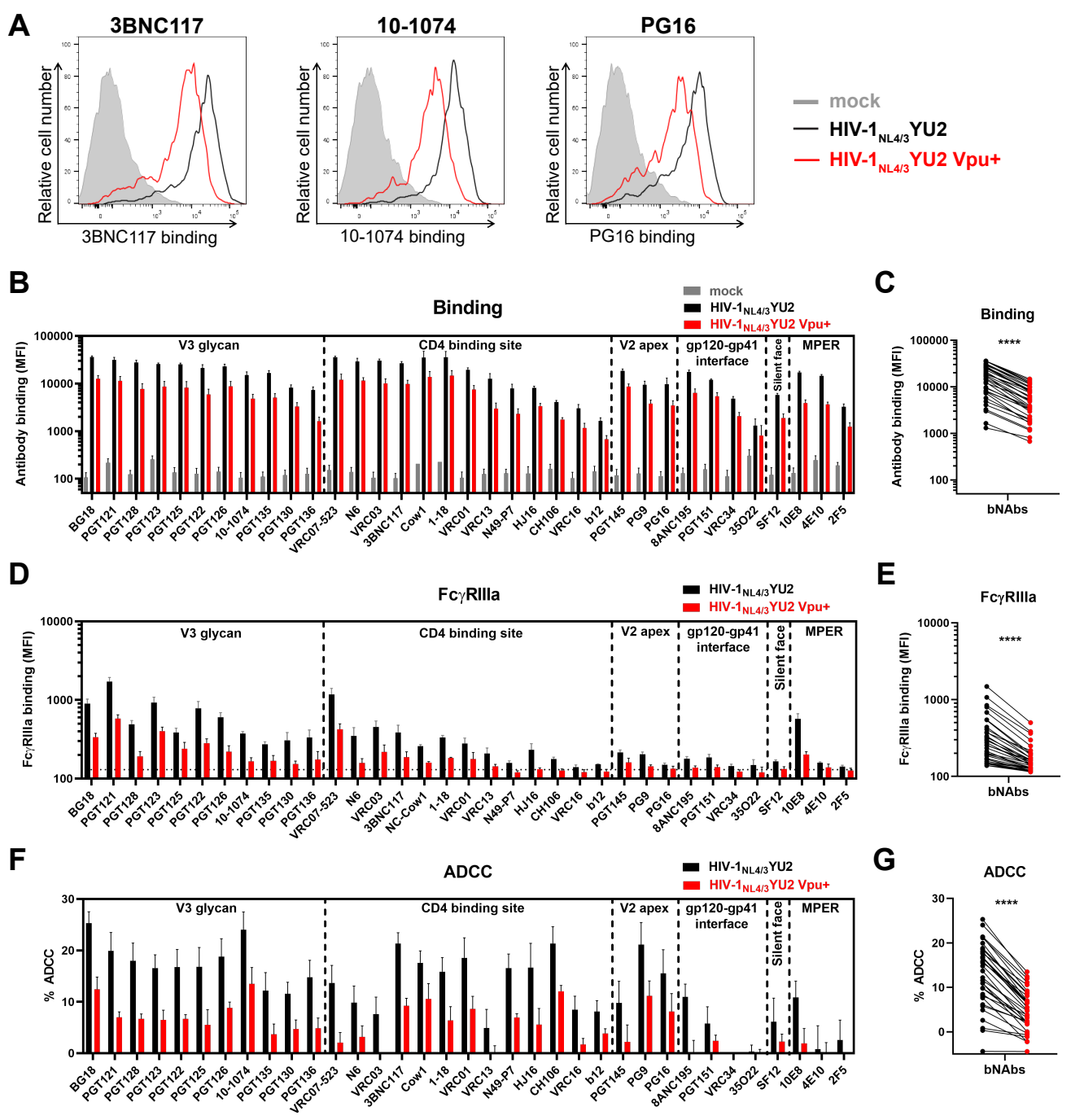
A
3BNC117
10-1074
PG16
Relative cell number
3BNC117 binding
10-1074 binding
PG16 binding
mock
HIV-1NL4/3YU2
HIV-1NL4/3YU2 Vpu+
B
Binding
Antibody binding (MFI)
V3 glycan
CD4 binding site
V2 apex
gp120-gp41 interface
Silent face
MPER
BG18 PGT121 PGT128 PGT123 PGT125 PGT122 PGT126 10-1074 PGT135 PGT130 PGT136 VRC07-523 N6 VRC03 3BNC117 Cow1 1-18 VRC01 VRC13 N49-P7 HJ16 CH106 VRC16 b12 PGT145 PG9 PG16 8ANC195 PGT151 VRC34 35O22 SF12 10E8 4E10 2F5
C
Binding
****
Antibody binding (MFI)
bNAbs
D
FcγRIIIa
FcγRIIIa binding (MFI)
BG18 PGT121 PGT128 PGT123 PGT125 PGT122 PGT126 10-1074 PGT135 PGT130 PGT136 VRC07-523 N6 VRC03 3BNC117 NC-Cow1 1-18 VRC01 VRC13 N49-P7 HJ16 CH106 VRC16 b12 PGT145 PG9 PG16 8ANC195 PGT151 VRC34 35O22 SF12 10E8 4E10 2F5
E
FcγRIIIa
****
FcγRIIIa binding (MFI)
bNAbs
F
ADCC
% ADCC
BG18 PGT121 PGT128 PGT123 PGT122 PGT125 PGT126 10-1074 PGT135 PGT130 PGT136 VRC07-523 N6 VRC03 3BNC117 Cow1 1-18 VRC01 VRC13 N49-P7 HJ16 CH106 VRC16 b12 PGT145 PG9 PG16 8ANC195 PGT151 VRC34 35O22 SF12 10E8 4E10 2F5
G
ADCC
****
% ADCC
bNAbs

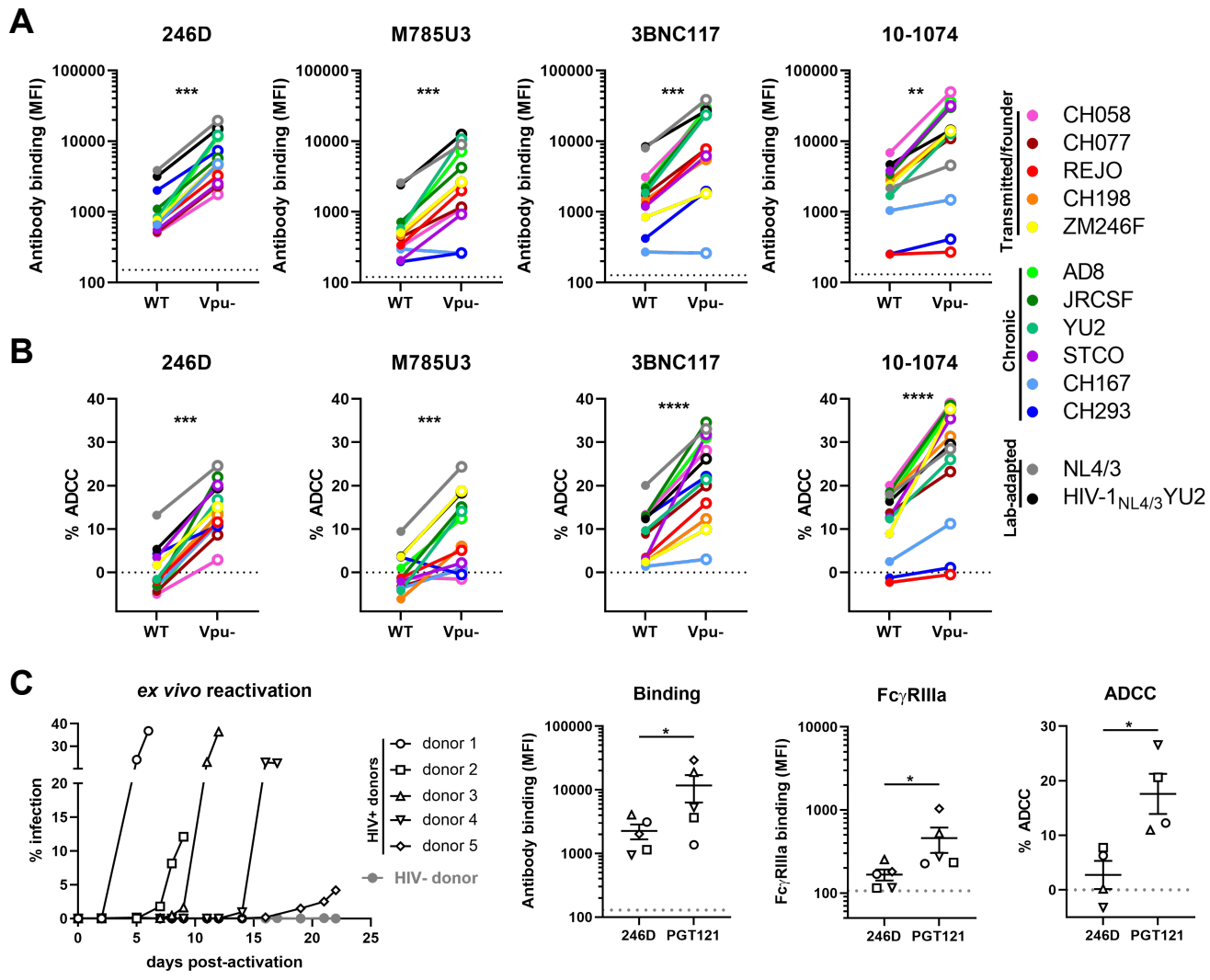
A
246D
M785U3
3BNC117
10-1074
Antibody binding (MFI)
100000
10000
1000
100
***
**
WT
Vpu-
Transmitted/founder
CH058
CH077
REJO
CH198
ZM246F
Chronic
AD8
JRCSF
YU2
STCO
CH167
CH293
Lab-adapted
NL4/3
HIV-1NL4/3YU2
B
% ADCC
40
30
20
10
0
****
C
ex vivo reactivation
% infection
days post-activation
HIV+ donors
donor 1
donor 2
donor 3
donor 4
donor 5
HIV- donor
Binding
FcγRIIIa
ADCC
246D
PGT121
FcγRIIIa binding (MFI)

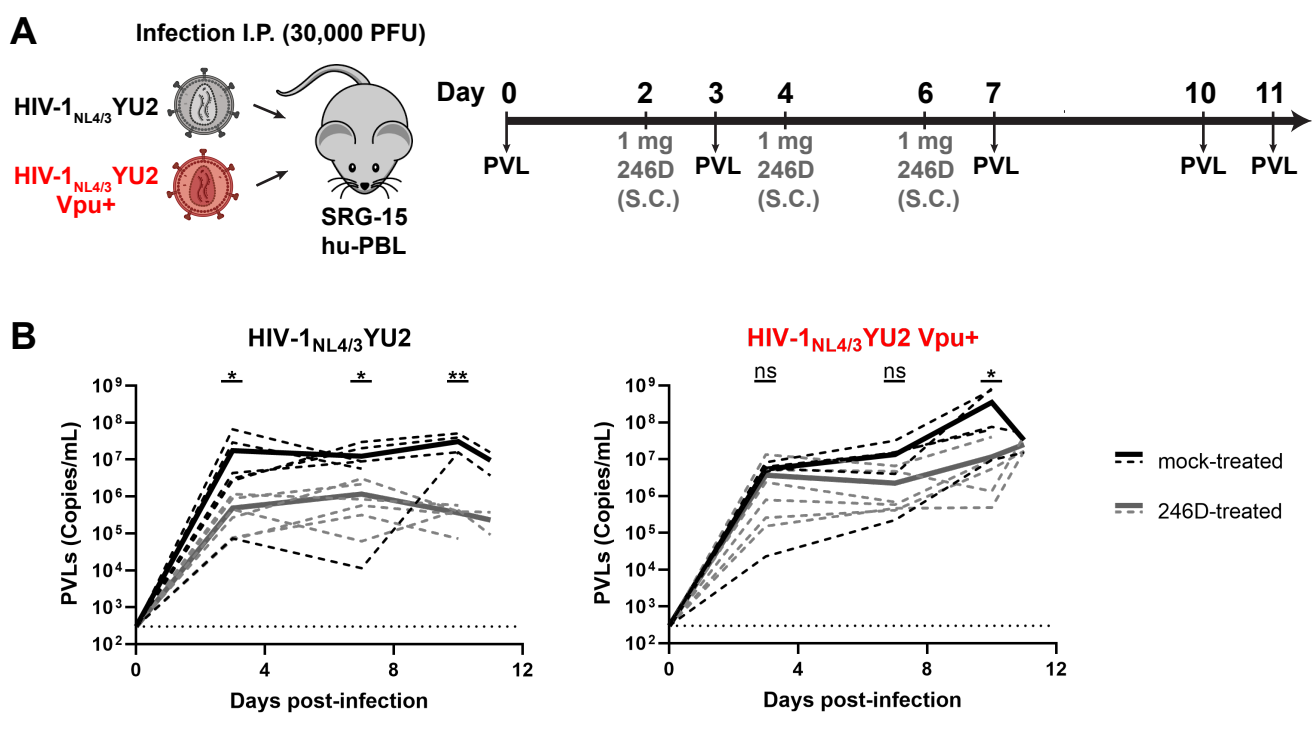
A
Infection I.P. (30,000 PFU)
HIV-1NL4/3YU2
HIV-1NL4/3YU2 Vpu+
SRG-15 hu-PBL
Day 0 2 3 4 6 7 10 11
PVL
1 mg 246D (S.C.)
PVL
1 mg 246D (S.C.)
PVL
1 mg 246D (S.C.)
PVL
PVL
PVL
B
HIV-1NL4/3YU2
HIV-1NL4/3YU2 Vpu+
PVLs (Copies/mL)
Days post-infection
*
*
**
ns
ns
*
mock-treated
246D-treated

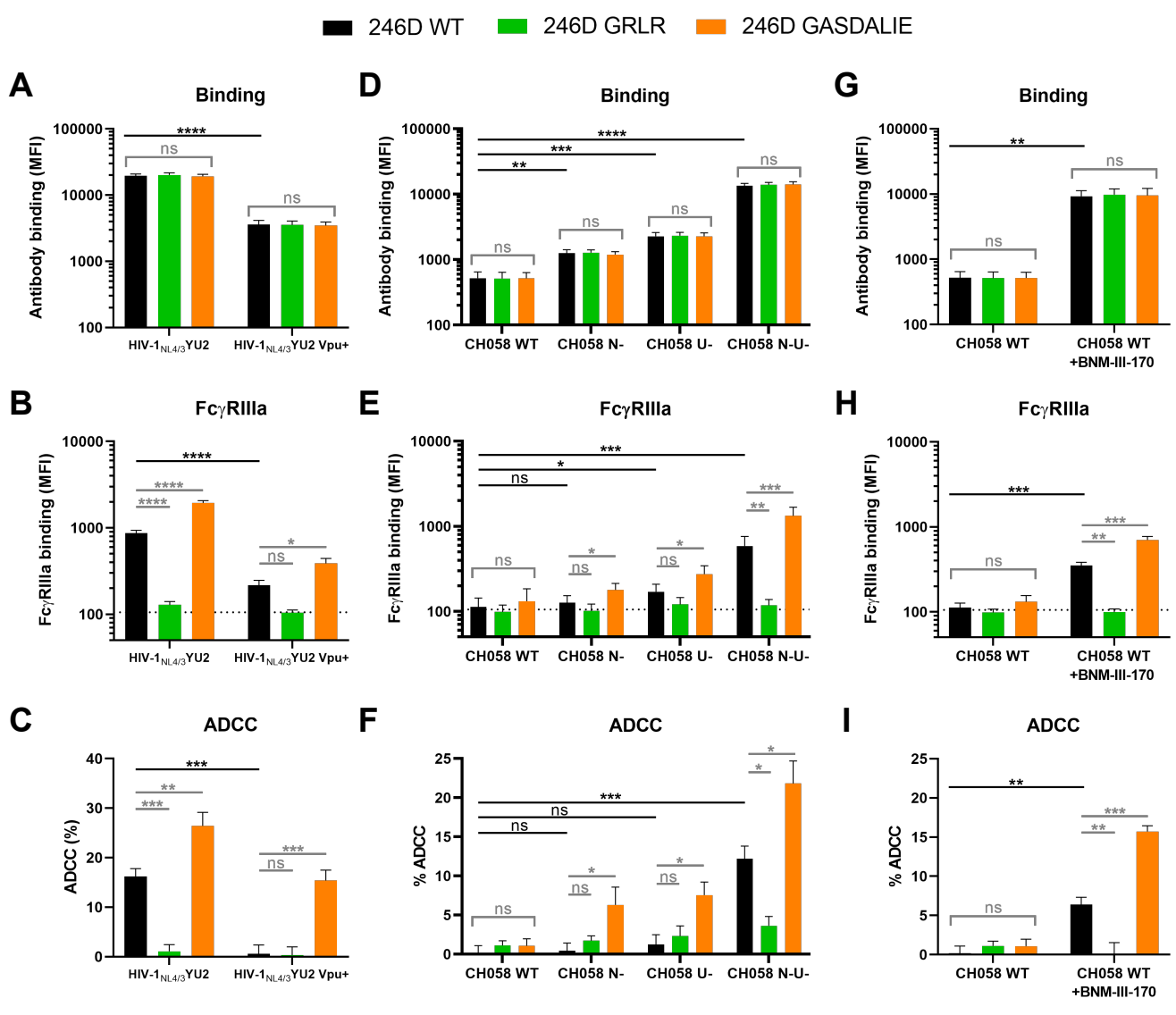
246D WT
246D GRLR
246D GASDALIE
A
Binding
Antibody binding (MFI)
HIV-1NL4/3YU2
HIV-1NL4/3YU2 Vpu+
B
FcγRIIIa
FcγRIIIa binding (MFI)
C
ADCC
ADCC (%)
D
CH058 WT
CH058 N-
CH058 U-
CH058 N-U-
E
% ADCC
F
G
CH058 WT +BNM-III-170
H
I
ns

SUPPLEMENTAL FIGURE LEGENDS

Table S1. Cohort of HIV-1-infected individuals. Related to Figure 1.

Figure S1. Classification of anti-gp41 non-neutralizing antibodies in two main clusters. Related to Figures 3 and 5.

(**A**) The binding of Alexa Fluor 647 (AF647)-precoupled anti-gp41 cluster I F240 mAb or anti-gp41 cluster II 2.2B mAb was evaluated on HIV-$1_{NL4/3}$YU2-infected cells in presence of a panel of unlabeled anti-gp41 nnAbs to determine epitope cross-competition. A pool of purified immunoglobulins from HIV-1-infected individuals (HIV-IG) was used as a positive control. Monoclonal antibodies with known non-competing epitopes (3BNC117, 17b, 10E8) were used as negative controls. (**B**) Lentiviral particles were produced from HIV-$1_{NL4/3}$YU2 IMC expressing Vpu or not. Viruses were incubated with serial dilutions of anti-Env mAbs (246D, M785U3, 3BNC117, 10-1074) at 37°C for 1 h prior to infection of TZM-bl target cells. The infectivity at each Ab concentration tested is shown as the percentage of infection without Ab for each virus. Quadruplicate samples were analyzed in each experiment. The data shown are the means of results obtained in three independent experiments. Error bars indicate means ± the SEM. Neutralization half maximal inhibitory concentration (IC_{50}) values are summarized in (**C**).

Figure S2. Epitope specificity dictates anti-Env ADCC responses mediated by nnAbs and bNAbs. Related to Figures 3 and 4.

(**A-F**) Levels of antibody binding, FcγRIIIa binding and ADCC responses mediated by (**A-C**) nnAbs and (**D-F**) bNAbs as classified by epitope specificity (gp41 nnAbs, gp120 nnAbs; V3

glycan, CD4-binding site, V2 apex, gp120-gp41 interface, MPER). Statistical significance was tested using (**A-C**) an unpaired t test or a Mann-Whitney U test and (**D-F**) a one-way ANOVA with a Holm-Sidak post-test or a Kruskal-Wallis test with a Dunn's post-test based on statistical normality (*, $P < 0.05$; **, $P < 0.01$; ***, $P < 0.001$; ****, $P < 0.0001$; ns, nonsignificant).

Figure S3. Monoclonal antibody 246D recognizes a gp41 linear peptide occluded in the closed Env trimer. Related to Figure 7.

(**A**) Logo depiction of the frequency of each amino acid from the HIV-1 Env gp41 C-C loop region (residues 583-618) in all HIV-1 isolates. The height of the letter indicates its frequency among all strains. The 2019 Los Alamos database-curated filtered web Env alignment was used as the basis for this figure, which contains 6,223 individual Env amino acid sequences. Residue numbering is based on the HXB2 reference strain of HIV-1. (**B**) Indirect ELISA was performed using HIV-1 Env gp41 peptides corresponding to the C-C loop region, or a SARS-CoV-2 Spike S2 peptide as a negative control. Peptide-coated wells were incubated with anti-gp41 246D and F240 mAbs, as well as anti-gp120 cluster A A32 mAb as a negative control. Antibody binding was detected using HRP-conjugated anti-human IgG and was quantified by relative light units (RLU). The data shown are the means of results obtained in three independent experiments. Error bars indicate means ± the SEM**.** (**C**) 246D binding affinity and kinetics to gp41 C-C loop using surface plasmon resonance (SPR). The 246D IgG was immobilized as the ligand on a Protein A chip and HIV-1 gp41 (583-618) peptide used as analyte from 0.488 to 31.25 nM (2-fold serial dilution). Kinetic constants were determined using a 1:1 Langmuir model in bimolecular interaction analysis (BIA) evaluation software (experimental readings depicted in black and fitted curves in red). (**D-E**) Mapping of the ^{596}WGCSGKLICTT^{606} epitope within available structures of HIV-1 Env. (**D**) The

closed conformation of HIV-1 Env (PDB: 6ULC) (Pan et al., 2020) from a cryo-EM structure of full-length HIV-1 Env bound to the Fab of the antibody PG16 (not shown), with the 246D epitope highlighted in red. The 246D epitope is fully occluded in the closed the trimer and not accessible for antibody binding. (**E**) The CD4-triggered HIV-1 Env trimer (PDB: 3J70) (Rasheed et al., 2015) from a computational model of full-length HIV-1 Env bound to the d1d2 domain of CD4 and the Fab of antibody 17b (not shown). In the CD4 triggered trimer the 246D epitope is largely disordered (highlighted with a broken red line for one of three gp41 protomers), but it is exposed at the surface of trimer and available for antibody recognition.

REFERENCES

Pan, J., Peng, H., Chen, B., and Harrison, S.C. (2020). Cryo-EM Structure of Full-length HIV-1 Env Bound With the Fab of Antibody PG16. J Mol Biol *432*, 1158-1168.

Rasheed, M., Bettadapura, R., and Bajaj, C. (2015). Computational Refinement and Validation Protocol for Proteins with Large Variable Regions Applied to Model HIV Env Spike in CD4 and 17b Bound State. Structure *23*, 1138-1149.

Table S1. Cohort of HIV-1-infected individuals

Group	Gender		Age (years)[a]	Days since infection[a]	Days since ART[a]	Days between infection and ART[a]	Viral load (copies/mL)[a]	CD4 count (cells/mm^3)[a]
	Male	Female						
Group 1 0-90 days untreated	10	0	40 [18-55]	68 [42-97]	N/A	N/A	60848 [132-391113]	470 [430-829]
Group 2 91-180 days untreated	10	0	38 [20-58]	135 [109-177]	N/A	N/A	21663 [6641-195302]	650 [420-1235]
Group 3 181-365 days untreated	10	0	31 [24-45]	240 [203-314]	N/A	N/A	27785 [1866-260852]	490 [230-770]
Group 4 2-5 years untreated	11	1	36 [23-54]	1158 [856-1810]	N/A	N/A	29234 [14255-809600]	421 [200-1311]
Group 5 2-5 years ART-treated	7	1	37 [23-60]	983 [794-1570]	690 [19-879]	428 [192-986]	50 [40-3337]	615 [170-1149]

[a]Values shown are group medians with ranges in bracket.

ART: antiretroviral therapy
N/A: not applicable

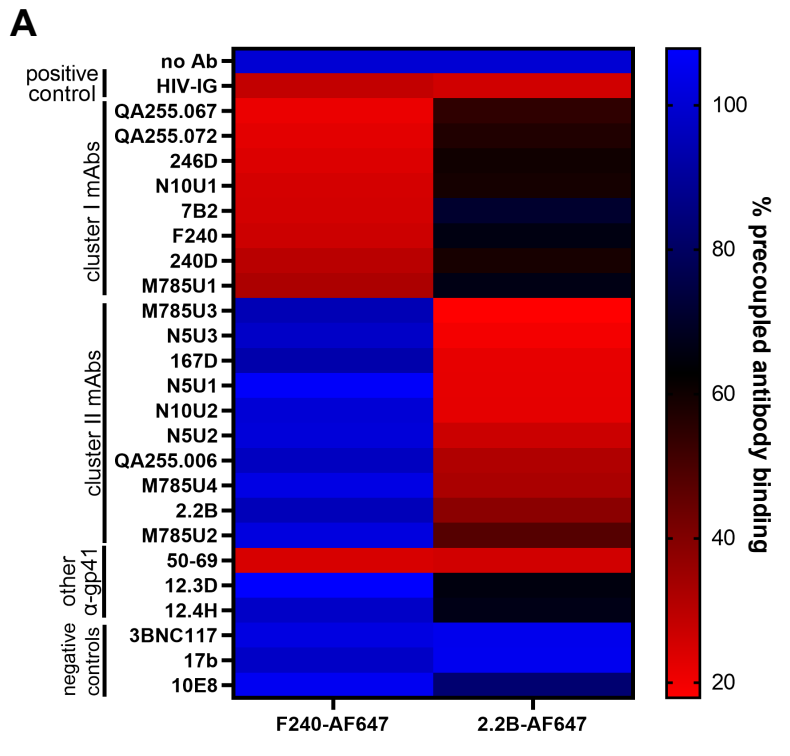

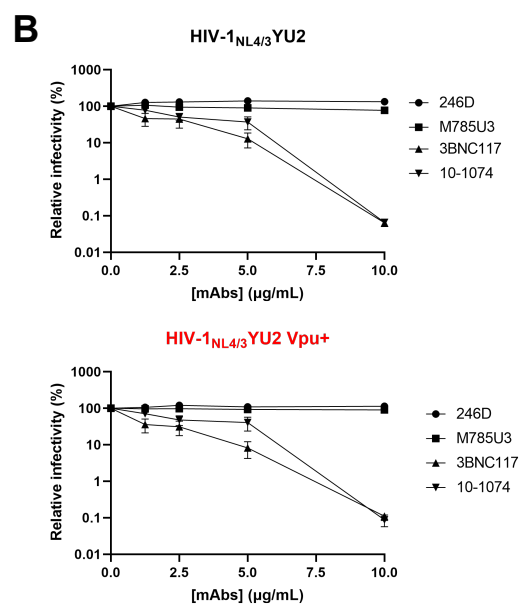

C

Virus	Neutralization IC_{50} (μg/mL)			
	246D	M785U3	3BNC117	10-1074
HIV-$1_{NL4/3}$YU2	>10	>10	0.738	3.063
HIV-$1_{NL4/3}$YU2 Vpu+	>10	>10	0.645	3.062

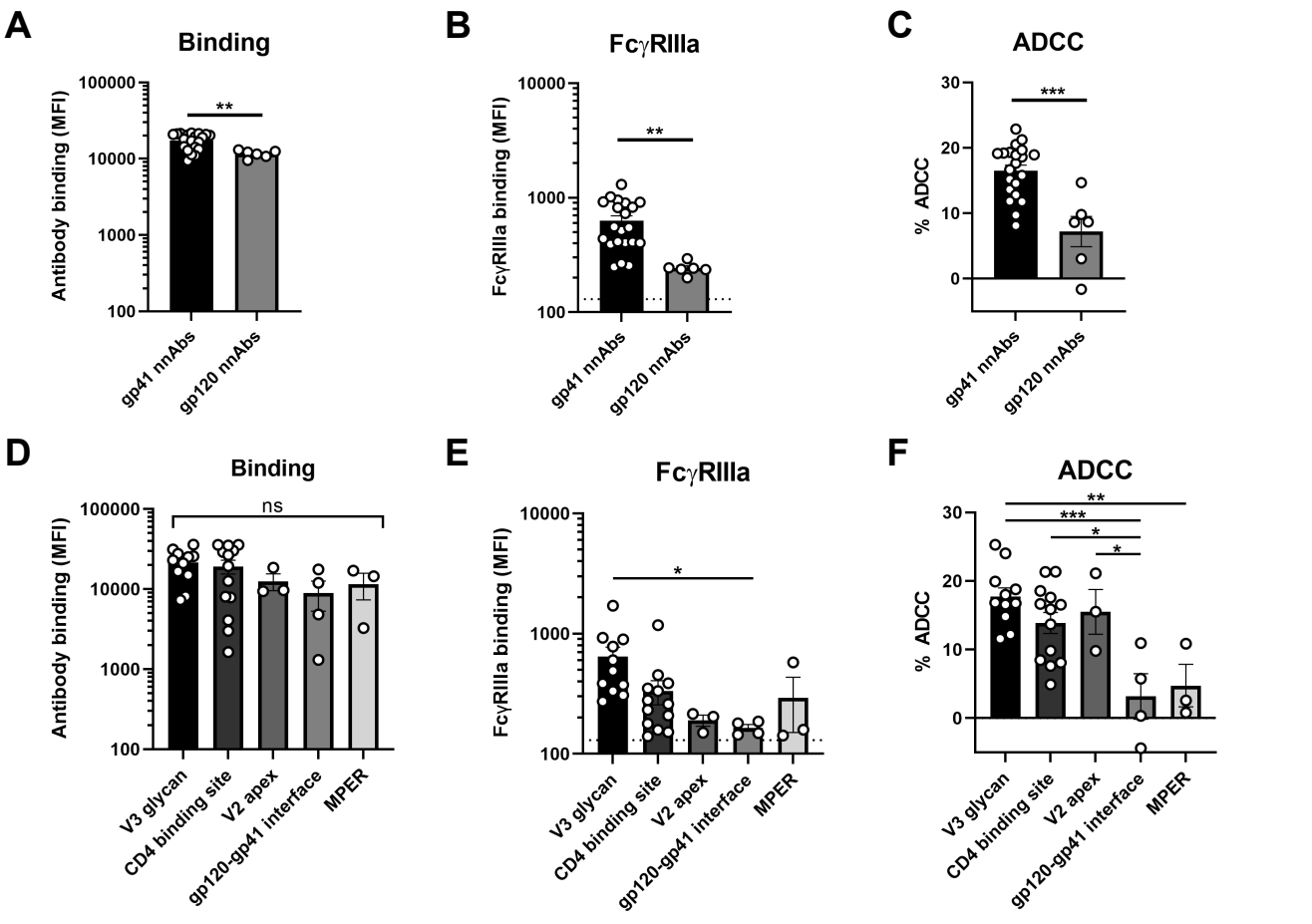
A
Binding
Antibody binding (MFI)
100000
10000
1000
100
**
gp41 nnAbs
gp120 nnAbs
B
FcγRIIIa
FcγRIIIa binding (MFI)
10000
1000
100
**
gp41 nnAbs
gp120 nnAbs
C
ADCC
% ADCC
30
20
10
0
***
gp41 nnAbs
gp120 nnAbs
D
Binding
Antibody binding (MFI)
100000
10000
1000
100
ns
V3 glycan
CD4 binding site
V2 apex
gp120-gp41 interface
MPER
E
FcγRIIIa
FcγRIIIa binding (MFI)
10000
1000
100
*
V3 glycan
CD4 binding site
V2 apex
gp120-gp41 interface
MPER
F
ADCC
% ADCC
30
20
10
0
**
***
*
*
V3 glycan
CD4 binding site
V2 apex
gp120-gp41 interface
MPER

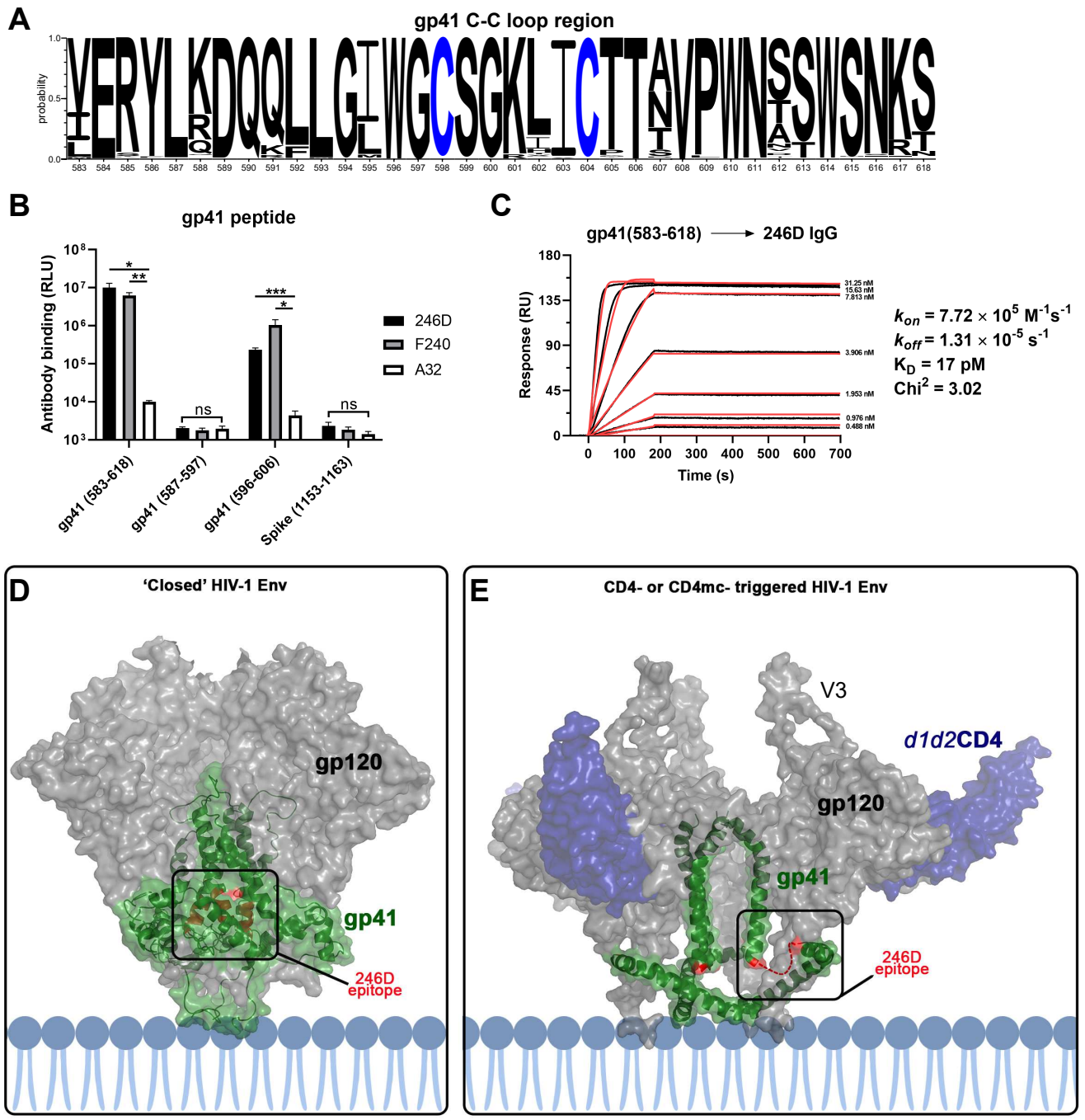
A
gp41 C-C loop region
probability
1.0
0.5
0.0
583 584 585 586 587 588 589 590 591 592 593 594 595 596 597 598 599 600 601 602 603 604 605 606 607 608 609 610 611 612 613 614 615 616 617 618
B
gp41 peptide
Antibody binding (RLU)
246D
F240
A32
*
**
***
*
ns
ns
gp41 (583-618)
gp41 (587-597)
gp41 (596-606)
Spike (1153-1163)
C
gp41(583-618) → 246D IgG
Response (RU)
Time (s)
31.25 nM
15.63 nM
7.813 nM
3.906 nM
1.953 nM
0.976 nM
0.488 nM
k_{on} = 7.72 × 10^5 M^{-1}s^{-1}
k_{off} = 1.31 × 10^{-5} s^{-1}
K_D = 17 pM
Chi^2 = 3.02
D
'Closed' HIV-1 Env
gp120
gp41
246D epitope
E
CD4- or CD4mc- triggered HIV-1 Env
V3
d1d2CD4
gp120
gp41
246D epitope